

## Temperature and Water Levels Collectively Regulate Methane Emissions From Subtropical Freshwater Wetlands

Global Biogeochemical Cycles

He, Keqi; Li, Wenhong; Zhang, Yu; Zeng, Angela; de Graaf, Inge E.M. et al

<https://doi.org/10.1029/2024GB008372>

This publication is made publicly available in the institutional repository of Wageningen University and Research, under the terms of article 25fa of the Dutch Copyright Act, also known as the Amendment Taverne.

Article 25fa states that the author of a short scientific work funded either wholly or partially by Dutch public funds is entitled to make that work publicly available for no consideration following a reasonable period of time after the work was first published, provided that clear reference is made to the source of the first publication of the work.

This publication is distributed using the principles as determined in the Association of Universities in the Netherlands (VSNU) 'Article 25fa implementation' project. According to these principles research outputs of researchers employed by Dutch Universities that comply with the legal requirements of Article 25fa of the Dutch Copyright Act are distributed online and free of cost or other barriers in institutional repositories. Research outputs are distributed six months after their first online publication in the original published version and with proper attribution to the source of the original publication.

You are permitted to download and use the publication for personal purposes. All rights remain with the author(s) and / or copyright owner(s) of this work. Any use of the publication or parts of it other than authorised under article 25fa of the Dutch Copyright act is prohibited. Wageningen University & Research and the author(s) of this publication shall not be held responsible or liable for any damages resulting from your (re)use of this publication.

For questions regarding the public availability of this publication please contact [openaccess.library@wur.nl](mailto:openaccess.library@wur.nl)

# Global Biogeochemical Cycles®

## RESEARCH ARTICLE

10.1029/2024GB008372

## Temperature and Water Levels Collectively Regulate Methane Emissions From Subtropical Freshwater Wetlands

Keqi He<sup>1</sup> , Wenhong Li<sup>1</sup> , Yu Zhang<sup>2</sup> , Angela Zeng<sup>3</sup>, Inge E. M. de Graaf<sup>4</sup> , Maricar Aguilos<sup>5</sup> , Ge Sun<sup>6</sup> , Steven G. McNulty<sup>6</sup>, John S. King<sup>5</sup> , Neal E. Flanagan<sup>7</sup>, and Curtis J. Richardson<sup>7</sup>

### Key Points:

- Random forest models trained on FLUXNET-CH4 data were used to identify key variables and estimate subtropical wetland methane emissions
- Variable importance analysis suggested that temperature and water levels together dominate subtropical freshwater wetland methane emissions
- A high-resolution (~1 km × 1 km) and long-term (1982–2010) wetland methane emission data set was developed for the Southeastern US

### Supporting Information:

Supporting Information may be found in the online version of this article.

### Correspondence to:

K. He,  
keqi.he@duke.edu

### Citation:

He, K., Li, W., Zhang, Y., Zeng, A., de Graaf, I. E. M., Aguilos, M., et al. (2025). Temperature and water levels collectively regulate methane emissions from subtropical freshwater wetlands. *Global Biogeochemical Cycles*, 39, e2024GB008372. <https://doi.org/10.1029/2024GB008372>

Received 24 SEP 2024

Accepted 16 FEB 2025

### Author Contributions:

**Conceptualization:** Keqi He, Wenhong Li

**Data curation:** Keqi He, Angela Zeng,

Inge E. M. de Graaf, Maricar Aguilos

**Formal analysis:** Keqi He, Angela Zeng

**Funding acquisition:** Wenhong Li

**Investigation:** Keqi He, Angela Zeng

**Methodology:** Keqi He, Wenhong Li

**Project administration:** Wenhong Li

**Resources:** Keqi He, Wenhong Li

**Software:** Keqi He, Angela Zeng

**Supervision:** Wenhong Li

**Validation:** Keqi He

**Visualization:** Keqi He

**Writing – original draft:** Keqi He

**Writing – review & editing:** Keqi He,

Wenhong Li, Yu Zhang, Angela Zeng,

Inge E. M. de Graaf, Maricar Aguilos,

Ge Sun, Steven G. McNulty, John S. King,

Neal E. Flanagan, Curtis J. Richardson

<sup>1</sup>Earth and Climate Sciences, Nicholas School of the Environment, Duke University, Durham, NC, USA, <sup>2</sup>Earth and Environmental Sciences Division, Los Alamos National Laboratory, Los Alamos, NM, USA, <sup>3</sup>Nicholas School of the Environment, Duke University, Durham, NC, USA, <sup>4</sup>Earth Systems and Global Change Group, Wageningen University & Research, Wageningen, The Netherlands, <sup>5</sup>Department of Forestry and Environmental Resources, North Carolina State University, Raleigh, NC, USA, <sup>6</sup>Eastern Forest Environmental Threat Assessment Center, USDA Forest Service Southern Research Station, USDA Forest Service, Raleigh, NC, USA, <sup>7</sup>Duke University Wetland Center, Nicholas School of the Environment, Duke University, Durham, NC, USA

**Abstract** Wetlands are the largest and most climate-sensitive natural sources of methane. Accurately estimating wetland methane emissions involves reconciling inversion (“top-down”) and process-based (“bottom-up”) models within the global methane budget. However, estimates from these two model types are inherently interdependent and often reveal substantial discrepancies. To enhance the reliability of both approaches, we need a comprehensive understanding of wetland methane emissions and an independent high-resolution long-term flux data set. Here, we employed a data-driven random forest approach to identify key variables influencing methane emissions from subtropical freshwater wetlands in the Southeastern United States. The model-estimated monthly mean methane fluxes fit well with measured methane fluxes ( $R^2 = 0.67$ ) at four representative FLUXNET-CH4 wetland sites across the region. Variable importance analysis highlighted the sensitivity of subtropical freshwater wetland methane emissions to variations in both temperature and water levels. High temperatures facilitate methanogenesis by enhancing microbial activities, while elevated water levels maintain anaerobic conditions necessary for methane production. Notably, the response of methane emissions to water level fluctuations is contingent on temperature conditions, and vice versa. Moreover, we constructed the first high-spatial-resolution (~1 km × 1 km) and long-term (1982–2010) gridded regional wetland methane flux product for the Southeastern United States, estimating annual methane emissions from subtropical freshwater wetlands in the region at  $4.93 \pm 0.11$  Tg CH<sub>4</sub> yr<sup>-1</sup> for 1982–2010. This new benchmark product holds promise for validating and parameterizing uncertain wetland methane emission processes in bottom-up models and provides improved prior information for top-down models.

## 1. Introduction

Methane (CH<sub>4</sub>) ranks as the second most impactful greenhouse gas (GHG) after carbon dioxide (CO<sub>2</sub>). The greenhouse effect of CH<sub>4</sub> is about 28 times that of CO<sub>2</sub> on a 100-year time horizon (IPCC, 2021). In recent years, the concentration of methane in the atmosphere has nearly tripled since preindustrial times (preindustrial level ~700 ppb), reaching over 1,930 ppb (Lan et al., 2024), which contributes 20%–30% of climate warming since the Industrial Revolution.

Of the various methane sources, wetlands stand out as the largest and most climate-sensitive natural source (Bartlett & Harriss, 1993; Huang et al., 2021; Wuebbles & Hayhoe, 2002; Zhu et al., 2013), contributing about 20%–30% to global methane emissions (Reddy & DeLaune, 2008; Saunio et al., 2020). The quantity of CH<sub>4</sub> released from wetland soils is dictated by the interplay of complex and competing processes, methane production and oxidation, which are primarily controlled by climatic and hydrological regimes (Bloom et al., 2010; Dai et al., 2012; Richardson et al., 2022, 2023; Saunio et al., 2020). Dramatic hydroclimatic changes, such as rising sea levels, increasing temperatures, and changing rainfall patterns, directly impact the microbial communities involved in methane production and consumption (Andersen et al., 2013; Mohanty et al., 2007; Yvon-Durocher et al., 2014; Zinder et al., 1984), influencing wetland CH<sub>4</sub> emissions in both magnitude and temporal fluctuations (Friborg et al., 1997; Whalen & Reeburgh, 1992; Zhu et al., 2013; Zimov et al., 2006). For example, rising sea levels drown coastal freshwater wetlands (He et al., 2022; Schuerch et al., 2018; Thorne et al., 2018), resulting in

oxygen depletion and facilitating methanogenesis. Meanwhile, higher temperatures can not only increase the rate of methane production but also enhance methane oxidation (Bansal et al., 2018; Rinne et al., 2018; L. Zhang et al., 2020). Therefore, determining the hydroclimatic controls on wetland CH<sub>4</sub> emissions is critical for improving our understanding and modeling of these emissions.

Existing estimates of wetland CH<sub>4</sub> emissions are primarily derived using either process-based models (“bottom-up”) (e.g., Andronova & Karol, 1993; Cao et al., 1996; Dai et al., 2012; Walter et al., 2001; H. Wang et al., 2023; Zhuang et al., 2004) or inversion models (“top-down”) (e.g., Bloom et al., 2017; Y. Zhang et al., 2021). However, the complex impacts of environmental variables, such as climate and hydrology, on wetland ecosystems introduce substantial uncertainty in estimating CH<sub>4</sub> fluxes (Chang et al., 2019). For example, using an ensemble of physically based land surface models, Saunio et al. (2020) quantified global wetland CH<sub>4</sub> emissions for 2008–2017 to be 149 Tg CH<sub>4</sub> yr<sup>-1</sup>, with an uncertainty range of 102–182 Tg CH<sub>4</sub> yr<sup>-1</sup>. In contrast, inversion models estimated emissions for the same period to be 181 Tg CH<sub>4</sub> yr<sup>-1</sup> (range 159–200 Tg CH<sub>4</sub> yr<sup>-1</sup>). This discrepancy between bottom-up and top-down estimates, along with extensive variability, manifests the considerable uncertainty inherent in the present estimation of wetland CH<sub>4</sub> emissions (Peltola et al., 2019). This uncertainty stems from the fact that top-down inversion models rely on a priori information from bottom-up physics-based land surface models, which, in turn, require detailed knowledge of CH<sub>4</sub> production, consumption, and transportation processes, as well as an accurate representation of landscape heterogeneity (Bloom et al., 2017; Saunio et al., 2017). Despite growing comprehension of the environmental factors influencing wetland CH<sub>4</sub> fluxes (Bridgman et al., 2013; Chang et al., 2020, 2021; Keller et al., 2023; Knox et al., 2021), there persists a critical gap in understanding wetland methane emissions specific to climate zones, notably in subtropical regions. Additionally, the size and distribution of wetlands vary widely across landscapes, influencing methane emission dynamics, yet are often inadequately captured in process-based and inversion models. Consequently, gaining an enhanced understanding of wetland methane emissions and the pivotal environmental factors governing them in subtropical regions, along with developing an observation-based high-spatial-resolution wetland CH<sub>4</sub> flux product that accounts for these landscape-level variations, is crucial for addressing these gaps. This will improve the spatial representation and refine the parameterization of both bottom-up and top-down models.

The Southeastern (SE) United States (US) is home to nearly half of the total wetlands in the contiguous US (Dahl, 2011; Trettin et al., 2020). More importantly, based on the remotely sensed CH<sub>4</sub> product, Carbon Monitoring System (CMS) Methane Flux for North America, subtropical wetlands in the SE US, especially in Florida and Louisiana, are hot spots for methane emissions within the conterminous US (Figure S1 in Supporting Information S2). However, compared to high-latitude peatlands (e.g., Peltola et al., 2019; Zhu et al., 2013), our understanding of the key environmental factors governing CH<sub>4</sub> emissions from subtropical wetlands in the SE US, as well as estimates of these emissions, especially high-resolution spatial estimates, remains relatively limited. The lack of systematic, high-spatial-resolution, and long-term CH<sub>4</sub> flux estimations has hampered our ability to accurately constrain CH<sub>4</sub> emissions from the dynamic subtropical wetland ecosystems across the SE US.

Over the last two decades, there has been a growing prevalence of eddy covariance (EC) measurements of wetland CH<sub>4</sub> emissions with the rapid advancement in sensor technology (e.g., Peltola et al., 2014). EC towers can continuously record CH<sub>4</sub> flux measurements along with meteorological variables such as air temperature, precipitation, vapor pressure deficit, incoming shortwave radiation, and wind speed. The emergence of global EC measurement networks such as FLUXNET and FLUXNET-CH<sub>4</sub> makes EC flux synthesis studies possible (Baldocchi, 2014; Baldocchi et al., 2001; Delwiche et al., 2021; McNicol et al., 2023; Pastorello et al., 2020). For example, machine learning (ML) models have been employed to scale up FLUXNET observations for modeling terrestrial carbon dioxide budgets (Beer et al., 2010; Jung et al., 2010, 2011, 2017). The knowledge learned from these studies, including factors affecting terrestrial ecosystem CO<sub>2</sub> production and emissions and the spatial distribution of CO<sub>2</sub> fluxes, are extensively utilized by the modeling community to assess the performance of process-based models (e.g., Wu et al., 2017) and to validate carbon products inversely derived from satellite observations (e.g., Sun et al., 2017; Y. Zhang et al., 2017).

Given these facts, we opt to use an ML approach to develop an observation-based high-spatial-resolution (0.0083° × 0.0083°, approximately 1 km × 1 km at the Equator) gridded data product of subtropical freshwater wetland CH<sub>4</sub> fluxes across the entire SE US from 1982 to 2010. Specifically, we aim first to use random forest (RF) regression models and FLUXNET-CH<sub>4</sub> measurements to identify the optimal relationships between subtropical freshwater wetland CH<sub>4</sub> fluxes and environmental factors. Driven by spatially explicit data of the

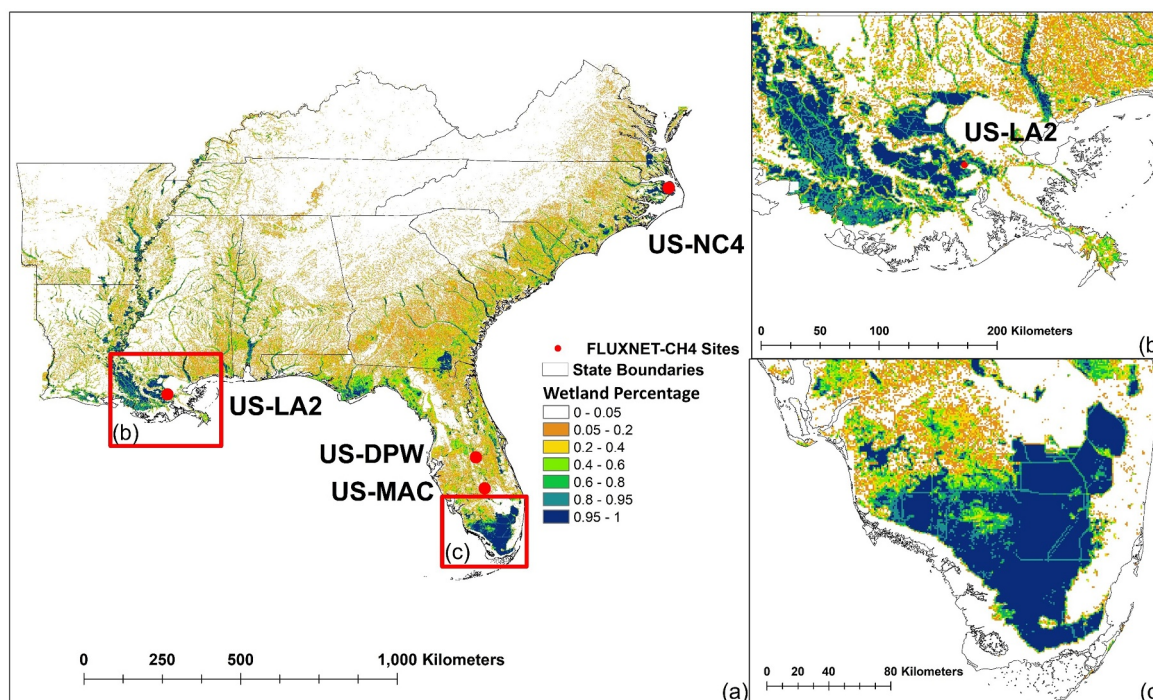


**Figure 1.** Spatial distribution of freshwater wetlands over (a) the Southeastern (SE) United States (US), (b) the Mississippi Delta, and (c) the Everglades, overlaid by four representative CH<sub>4</sub> flux observation sites (FLUXNET-CH<sub>4</sub> sites) used in this study and state boundaries. The wetland percentages at a spatial resolution of 0.0083° × 0.0083° were calculated from the National Wetlands Inventory (NWI).

dominant environmental variables, the developed RF regression model is then extrapolated to the entire SE US to estimate subtropical freshwater wetland CH<sub>4</sub> emissions in the region. To the best of our knowledge, this newly developed data set is the first high-spatial-resolution (~1 km × 1 km) and long-term (29 years from 1982 to 2010) gridded subtropical freshwater wetland CH<sub>4</sub> flux product for the SE US. The insights obtained from this study, including the identified key environmental control factors affecting subtropical freshwater wetland methane emissions, the spatial patterns of these emissions, and the characteristics of wetland methane flux variations at seasonal and annual scales, can improve our comprehension of the complex interplay among climate, hydrology, and wetland ecosystems. Additionally, these insights will aid in the development and refinement of process-based and inversion models for future wetland CH<sub>4</sub> flux upscaling studies.

## 2. Data and Methods

### 2.1. Study Area

This study focuses on subtropical freshwater wetland ecosystems in the SE US (Figure 1). The SE US, consisting of 11 states and spanning from the Appalachian Mountains to the Atlantic Ocean, is a unique region with extensive floodplains, wide coastal plains, and abundant rainfall, resulting in pervasive wetlands, particularly in the Mississippi Delta and the Everglades (Figure 1) (Hefner et al., 1994). Within this 1.52 million square kilometers region, about 9.4% (0.14 million km<sup>2</sup>) is subtropical freshwater wetlands. According to the National Wetlands Inventory (NWI), common freshwater wetland types in the SE US include freshwater forested/shrub wetlands (84.5%) and freshwater emergent wetlands (15.5%) (Dahl, 2011; Dahl & Stedman, 2013; Tiner, 1997; Wilen & Bates, 1995). These wetlands are mainly located along the Atlantic coast, the Mississippi River, and the Gulf of Mexico.

The climate conditions in the SE US are relatively uniform according to the Köppen-Geiger Climate Classifications (Beck et al., 2018, 2023; Kottek et al., 2006; Kriticos et al., 2012; Peel et al., 2007). Almost the entire SE US is classified as “Cfa” (Humid Subtropical: mild with no dry season, hot summer), except for a few parts of FL that are classified as “Cwa” (Humid Subtropical: dry winter, hot summer). Given that variations in wetland methane emissions are primarily determined by climatic and hydrological regimes (Bloom et al., 2010; Sauniois

et al., 2020), the hydroclimatic controls on methane emissions should be similar across all subtropical freshwater wetlands in the SE US.

## 2.2. Data Organization for Random Forest Model Development

Wetland methane flux measurements used in this study are from the FLUXNET-CH<sub>4</sub> Community Product, a global methane flux database compiled by standardizing and post-processing (i.e., partitioning and gap-filling) available Eddy Covariance (EC) CH<sub>4</sub> flux measurements (Delwiche et al., 2021; Knox et al., 2019). Within the SE US, four freshwater wetland sites (US-DPW, US-LA2, US-MAC, and US-NC4) exist (Figure 1 and Table 1). These sites cover common freshwater wetland types in the study area, including freshwater forested/shrub wetlands (US-NC4) and freshwater emergent wetlands (US-DPW, US-LA2, and US-MAC). The climatological means of air temperature and precipitation at these sites nearly span the range, as determined with a 95% confidence level, of air temperature (14.5–24.0°C) and precipitation (1,130–1,600 mm) observed in wetlands (wetland percentage >5%, Figure 1) within the SE US, respectively (Table 1). Consequently, these four sites represent the SE US subtropical freshwater wetlands reasonably well to create an upscaled subtropical freshwater wetland CH<sub>4</sub> flux product over the region based on EC data (see more discussion in Section 4.1).

The daily CH<sub>4</sub> fluxes used in this study were calculated as the means of gap-filled half-hourly observations collected at the four sites. Daily fluxes were retained only when at least 10 half-hourly (~20%) CH<sub>4</sub> observations were available. This gap-filling threshold was selected to retain as much data as possible while minimizing errors associated with filling long gaps (Dengel et al., 2013; McNicol et al., 2023; Peltola et al., 2019). The duration of daily CH<sub>4</sub> flux data varied across sites, ranging from a minimum of 433 days (US-LA2) to a maximum of 1,012 days (US-DPW). The data sets spanned between 2011 and 2017 (Figures S2–S5 in Supporting Information S2).

Fourteen explanatory variables, namely, air temperature ( $T_{\text{air}}$ ), precipitation (P), vapor pressure deficit (VPD), incoming shortwave radiation (SW\_IN), wind speed (WS), latent heat flux (LE), sensible heat flux (H), Palmer Drought Severity Index (PDSI), water level (WTL), leaf area index (LAI), the fraction of absorbed photosynthetically active radiation (fAPAR), gross primary productivity (GPP), net ecosystem exchange (NEE), and season were considered as potential drivers in our analysis (Table S1). These variables were chosen due to their anticipated direct or indirect impacts on wetland methane fluxes (Text S1 in Supporting Information S1; Chen et al., 2019; Huang et al., 2021; Knox et al., 2021; Oertel et al., 2016; Peltola et al., 2019; Sanches et al., 2019; Saunois et al., 2020; Savi et al., 2016; Zhu et al., 2013).

Among these variables, daily  $T_{\text{air}}$ , P, VPD, SW\_IN, WS, LE, H, GPP, and NEE were derived from half-hourly measurements recorded at the flux towers. Daily WTL was collected from different sources based on the coordinates of the sites. Specifically, WTL for US-DPW was obtained from a nearby groundwater monitoring well (POF-22 managed by the South Florida Water Management District Environmental Monitoring program) and adjusted to the site's specific elevation using NAVD88 as the vertical reference. WTL for US-LA2 were retrieved from the Coastwide Reference Monitoring System (co-located monitoring well CRMS2825-H01). WTL at US-MAC and US-NC4 were monitored on-site using ultrasonic water level dataloggers (Infinities, Port Orange, FL, USA; Aguilos et al., 2020, 2022). Monthly LAI and fAPAR were derived from the NOAA Climate Data Record (CDR) of Advanced Very High Resolution Radiometer (AVHRR) Surface Reflectance. Since “season” is a categorical variable, we used one-hot encoding to convert it into binary numerical variables to be used in the RF model (Davis, 2010; O'Grady & Medoff, 1988; Pedhazur & Kerlinger, 1982).

After collecting these 14 explanatory variables, we converted them all to a daily scale to resolve discrepancies in temporal resolutions among them (Table S1). Specifically, for monthly variables (PDSI, LAI, and fAPAR), we repeated the individual monthly values for each day of the month. Likewise, for the seasonal variable (season), each day within the same season was assigned the same value. Finally, we paired daily CH<sub>4</sub> fluxes with the corresponding daily values of the 14 potential drivers by time and location.

## 2.3. Random Forest Regression Models

Random forest (RF) regression models were set up in this study to establish the relationships between the explanatory variables (a.k.a. predictors) and subtropical freshwater wetland CH<sub>4</sub> fluxes (the response variable). The RF regression model, a type of bagging (Bootstrap AGgregation) algorithm, leverages ensemble learning

**Table 1**  
Description of the Eddy Covariance CH<sub>4</sub> Flux Tower Sites (FLUXNET-CH4 Sites) Used in This Study

Site ID	Name	Wetland type	Lat (°)	Lon (°)	Köppen climate class	MAT <sup>a</sup> (°C)	MAP <sup>b</sup> (mm)	MAMF <sup>c</sup> (nmol m <sup>-2</sup> s <sup>-1</sup> )	Fraction of gap-filled half-hourly methane fluxes (%)	Elevation <sup>d</sup> (m)	Soil type <sup>e</sup>	Reference
US-DPW	Disney Wilderness Preserve Wetland	Freshwater emergent wetlands	28.0521	-81.4361	Cwa <sup>f</sup>	22.6	1,142	159.0	26.2	23	Floridana mucky fine sand	Hinkle & Bracho, 2020
US-LA2	Salvador WMA Freshwater Marsh	Freshwater emergent wetlands	29.8587	-90.2869	Cfa <sup>g</sup>	20.2	1,655	142.5	56.2	0	Kenner muck	Holm et al., 2020
US-MAC	MacArthur Agro-Ecology	Freshwater emergent wetlands	27.1632	-81.1873	Cwa <sup>f</sup>	22.1	1,386	56.0	46.2	8	Immokalee sand	Sparks, 2020
US-NC4	NC_AlligatorRiver	Freshwater forested/shrub wetlands	35.7879	-75.9038	Cfa <sup>g</sup>	16.6	1,311	84.5	52.3	1	Hyde loam	Noormets et al., 2020

<sup>a</sup>MAT stands for "Mean Average Temperature." <sup>b</sup>MAP stands for "Mean Average Precipitation." <sup>c</sup>MAMF stands for "Mean Average Methane Fluxes." <sup>d</sup>The elevations of sites US-DPW, US-LA2, and US-NC4 were obtained from the FLUXNET website (<https://fluxnet.org/sites/site-list-and-pages/>), while the elevation of US-MAC was derived from Shuttle Radar Topography Mission data with a 1 arc-second spatial resolution. <sup>e</sup>The soil type for each site is based on the Web Soil Survey (<https://websoilsurvey.nrcs.usda.gov/app/WebSoilSurvey.aspx>). <sup>f</sup>Cwa represents "Humid Subtropical: mild with no dry season, hot summer." <sup>g</sup>Cfa represents "Humid Subtropical: dry winter, hot summer."

techniques (Altman & Krzywinski, 2017; Prasad et al., 2006). It constructs multiple decision trees, each trained on a random subset of the input training data and a random subset of explanatory variables. To make predictions, each decision tree independently generates a value, and the final prediction is the average of these individual values (Breiman, 2001). In flux upscaling studies, the accuracy of RF is superior to or par with other ML algorithms (Bodesheim et al., 2018; Tramontana et al., 2015; Xu et al., 2018). Additionally, RF models are interpretable, allowing us to rank the importance of each environmental variable based on its contribution to estimating wetland methane fluxes (He et al., 2023; Sulova & Jokar Arsanjani, 2020). Furthermore, the RF regression model is capable of mining the underlying relationships between explanatory variables and the response variable without requiring prior knowledge of these relationships. This is achieved by calculating the partial dependence (PD) between each predictor and the response variable after averaging out the effects of the other predictors (Friedman, 2001; Hastie et al., 2001):

$$f(X_i) = \frac{1}{n} \sum_{k=1}^n \text{RF}(x_1^k, \dots, x_i^k, \dots, x_m^k) \quad (1)$$

where  $x_i^k$  represents the  $k$ th sample of the  $i$ th independent predictor,  $m$  represents the number of predictors,  $n$  represents the number of samples, and  $\text{RF}(\cdot)$  represents the trained RF regression model. By plotting the PD against each key predictor, responses of wetland methane emissions to changes in the dominant predictors can be visualized (He et al., 2023; Zeng et al., 2017). Thus, the RF regression model is an appropriate data-driven model for reproducing the intricate dynamics between subtropical freshwater wetland  $\text{CH}_4$  fluxes and their dominant environmental factors (Sturtevant et al., 2016). This is particularly relevant in cases where precise prior knowledge of the links between subtropical freshwater wetland  $\text{CH}_4$  emissions and environmental factors is usually lacking.

To determine the optimal subset of predictors from the 14 candidate explanatory variables (see Section 2.2 and Table S1) and evaluate the performance of the RF regression model, we employed a forward feature selection approach combined with leave-one-group-out cross-validation (LOGOCV) (McNicol et al., 2023; Peltola et al., 2019). This method involves sequentially adding explanatory variables to the model one at a time and assessing model performance based on the highest average  $R^2$  (coefficient of determination) and the lowest average MAE (mean absolute error) achieved through LOGOCV. LOGOCV, previously used in the global/regional upscaling of  $\text{CO}_2$ ,  $\text{CH}_4$ , and energy fluxes, is well-suited for making spatio-temporal predictions from spatially sparse time series data (McNicol et al., 2023; Peltola et al., 2019; Roberts et al., 2017; Tramontana et al., 2016). Specifically, we constructed four individual RF models for each predictor set, training on data from three wetland sites and testing on the left-out site. This process was repeated iteratively with different subsets of predictors. Ultimately, the inclusion of SW\_IN, VPD,  $T_{\text{air}}$ , P, WS, WTL, and season as predictors resulted in the best-performing RF models, with the highest average  $R^2$  and lowest average MAE across the four models. After determining the optimal predictor subset, we fitted a final RF model using the complete data set from all four freshwater sites (totaling 3,105 site-days with complete  $\text{CH}_4$  fluxes and seven predictors) (Kuhn & Johnson, 2013; Roberts et al., 2017).

#### 2.4. Regional Extrapolation

We employed the developed RF regression model to map subtropical freshwater wetland  $\text{CH}_4$  emissions across the SE US at a spatial resolution of  $0.0083^\circ \times 0.0083^\circ$  ( $\sim 1 \text{ km} \times 1 \text{ km}$ ) for the period 1982–2010. The chosen spatial resolution aligns with the footprint of eddy covariance (EC) flux towers, which typically range from hundreds to thousands of meters in radius (Chu et al., 2021; Krauss et al., 2016). To extrapolate the RF model, we prepared spatially explicit gridded data for seven selected predictors. Climatic data, including daily SW\_IN, VPD,  $T_{\text{air}}$ , and P, were extracted and/or calculated from the Daymet data set (Thornton et al., 1997). These climatic data were originally in the spatial resolution of  $1 \text{ km} \times 1 \text{ km}$ . Daily WS data, with a spatial resolution of  $0.0625^\circ \times 0.0625^\circ$ , was sourced from Livenh et al. (2013). The monthly WTL for each  $0.083^\circ$  grid cell was obtained from simulations of a hydrological model developed by de Graaf et al. (2019). The regional extrapolation was constrained to 1982–2010 due to data availability, particularly the WTL data—only available through 2010 (de Graaf et al., 2019)—which restricted our ability to estimate  $\text{CH}_4$  emissions across the entire region beyond 2010.

To ensure consistent spatial ( $0.0083^\circ \times 0.0083^\circ$ ) and temporal (daily) resolutions, the climatic data from Daymet (SW\_IN, VPD,  $T_{\text{air}}$ , and P) were projected onto the “GCS\_WGS\_1984” coordinate system with a spatial resolution of  $0.0083^\circ \times 0.0083^\circ$  using the “Project Raster” function (Resampling Technique: NEAREST) under the “Data Management” Tool in ArcMap 10.5.1 (ArcGIS, 2016). As for the WS data, it was downsampled to  $0.0083^\circ \times 0.0083^\circ$  following Equations 5 and 6 as detailed in Y. Zhang et al. (2020). Lastly, the monthly WTL data were first spatially downsampled utilizing the following equation, and then the individual monthly WTL<sub>f</sub> values were repeated to represent each day within the corresponding month:

$$\text{WTL}_f = \text{WTL}_c - (\text{DEM}_f - \overline{\text{DEM}}) \quad (2)$$

where WTL<sub>f</sub> is the downsampled fine-resolution ( $0.0083^\circ \times 0.0083^\circ$ ) WTL, WTL<sub>c</sub> is the original coarse-resolution ( $0.083^\circ \times 0.083^\circ$ ) WTL, DEM<sub>f</sub> is the digital elevation model (DEM) value derived from the high-resolution 30 arcsec ( $0.0083^\circ$ ) HydroSHED (Lehner et al., 2008), and  $\overline{\text{DEM}}$  is the mean DEM value of 100 fine-resolution ( $0.0083^\circ \times 0.0083^\circ$ ) grids within the coarse-resolution ( $0.083^\circ \times 0.083^\circ$ ) grid where the targeted fine-resolution grid is located in.

After assembling the spatially explicit daily climatic, hydrological, and seasonality data, we used the developed RF regression model to estimate daily subtropical freshwater wetland methane fluxes across the entire SE US at the  $0.0083^\circ \times 0.0083^\circ$  spatial resolution. The daily subtropical freshwater wetland methane flux at each grid across the entire SE US was calculated as follows:

$$\text{Flux}_i = \text{Flux}_{i,\text{RF}} \times \text{Wetland}_i \quad (3)$$

where Flux<sub>i</sub> is the estimated methane flux at grid *i*, Flux<sub>i,RF</sub> is the RF model estimated methane fluxes at grid *i* if the whole grid is 100% covered by freshwater wetlands. Wetland<sub>i</sub> is the percentage of freshwater wetlands within the grid *i*.

To analyze seasonal and interannual dynamics of CH<sub>4</sub> emissions in SE US subtropical freshwater wetlands, we calculated the monthly and annual means of the daily upscaled data sets. Additionally, the standard deviation of the daily data sets for each month was used to quantify the variability in monthly CH<sub>4</sub> emissions. This approach enabled us to capture both the mean trends and the variability in CH<sub>4</sub> emissions over time.

## 2.5. Comparison With Top-Down and Bottom-Up Products

To validate our high-resolution, spatially distributed estimates of subtropical freshwater wetland methane fluxes across the SE US, we compared them with two existing methane flux products: the top-down Carbon Monitoring System (CMS) Methane Flux for North America product ( $0.5^\circ \times 0.667^\circ$ , Turner et al., 2015) and the bottom-up Global Wetland Methane Emissions derived from FLUXNET and the UpCH<sub>4</sub> Model (UpCH<sub>4</sub>,  $0.25^\circ \times 0.25^\circ$ , McNicol et al., 2023). Further details on these comparisons are provided in Text S2 in Supporting Information S1.

## 3. Results

### 3.1. Model Performance at the Observation Sites

The RF regression models, constructed using seven predictors (SW\_IN, VPD,  $T_{\text{air}}$ , P, WS, WTL, and season) and with 500 trees, most effectively reproduced the monthly mean CH<sub>4</sub> fluxes measured by the EC towers during leave-one-group-out cross-validation (LOGOCV). For the testing sites excluded from training, the average MAE and R<sup>2</sup> between the simulated and measured monthly mean wetland CH<sub>4</sub> fluxes were  $51.98 \text{ nmol m}^{-2} \text{ s}^{-1}$  and 0.67 ( $p < 0.0001$ ), respectively (Figures 2a–2d and Figure S6 in Supporting Information S2). Across the four individual RF models (each trained on data from three sites and tested on the left-out site), R<sup>2</sup> varied from 0.59 (US-MAC, Figure 2c) to 0.77 (US-LA2, Figure 2b), while MAE ranged from  $48.16 \text{ nmol m}^{-2} \text{ s}^{-1}$  (US-LA2, Figure 2b) to  $53.96 \text{ nmol m}^{-2} \text{ s}^{-1}$  (US-DPW, Figure 2a). Detailed comparisons between the estimated and measured wetland CH<sub>4</sub> fluxes at the daily scale for the four sites can be found in Figures S7 and S8 in Supporting Information S2. Overall, the RF regression models captured the observed CH<sub>4</sub> fluxes well at both daily and monthly scales across the four FLUXNET-CH<sub>4</sub> sites (Figures 2a–2d and Figures S6–S8 in Supporting Information S2).

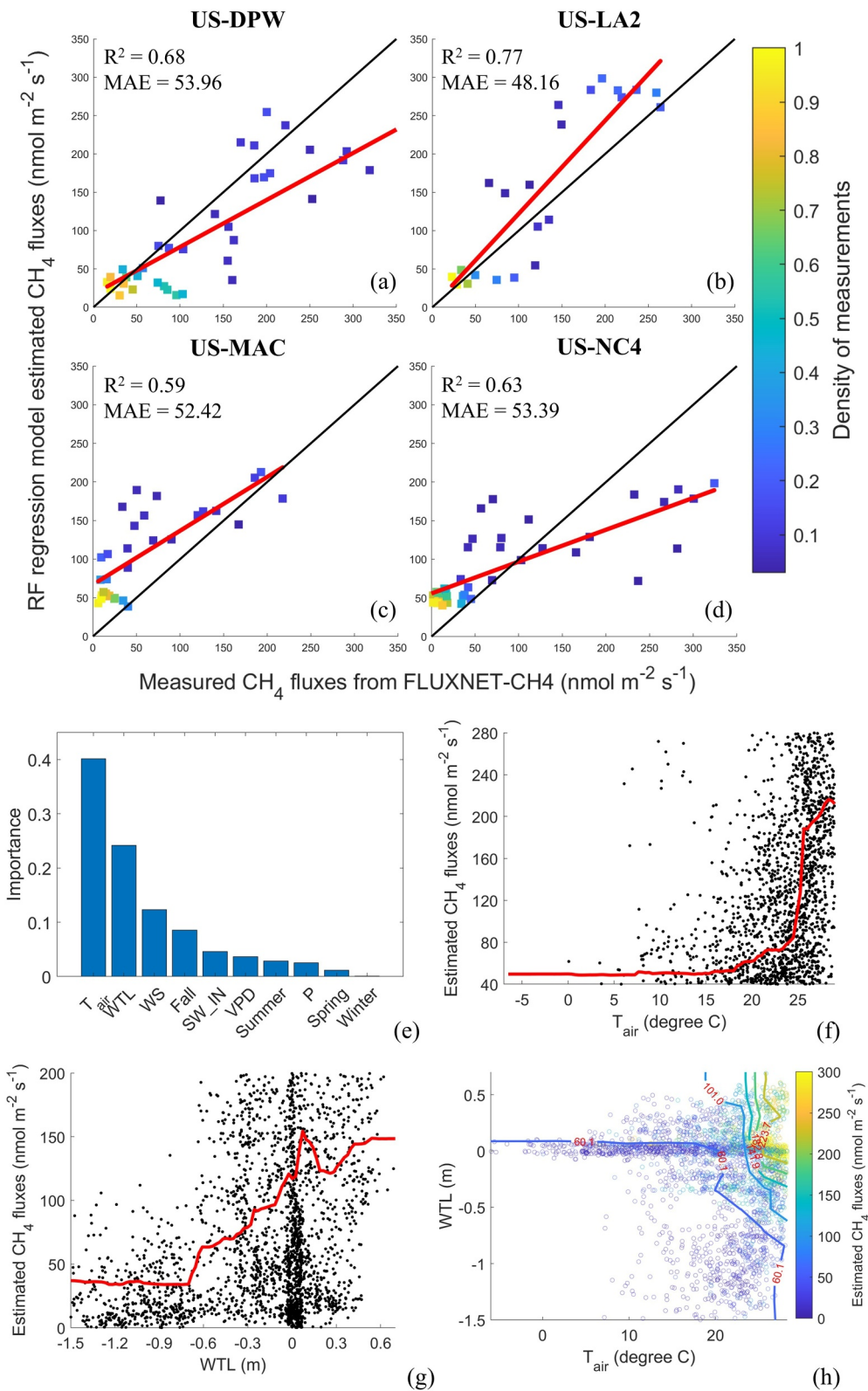


Figure 2.

After determining the optimal predictors (SW\_IN, VPD,  $T_{\text{air}}$ , P, WS, WTL, and season) and fine-tuning the hyperparameters of the RF regression models (500 trees), we proceeded to train a final RF regression model using all available data from the four sites. All results presented in the subsequent sections were derived from this final RF model.

### 3.2. Key Variables Affecting Wetland Methane Fluxes

Figure 2e ranks the importance of each variable in estimating subtropical freshwater wetland methane emissions based on Gini importance values. The variable with the highest Gini importance value for subtropical freshwater wetland methane fluxes was  $T_{\text{air}}$  (0.40), followed by WTL (0.24). These high Gini importance values indicated that methane emissions from SE US subtropical freshwater wetlands were primarily influenced by air temperature ( $T_{\text{air}}$ ) and water levels (WTL). To further elucidate how dominant predictors,  $T_{\text{air}}$  and WTL, impacted subtropical freshwater wetland methane emissions, we plotted the partial dependence (PD) of wetland methane fluxes on  $T_{\text{air}}$ , WTL, and  $T_{\text{air}}$  and WTL combined, separately (Figures 2f–2h).

Figure 2f reveals a sigmoidal response of wetland methane fluxes to  $T_{\text{air}}$ , with 24°C and 28°C marking the lower and upper thresholds, respectively. Within this range, an increase in  $T_{\text{air}}$  leads to a disproportionate enhancement of wetland  $\text{CH}_4$  emissions.

Figure 2g shows the influence of WTL on wetland  $\text{CH}_4$  emissions. Generally, wetland  $\text{CH}_4$  fluxes increase with increasing WTL. When WTL is below  $-0.7$  m,  $\text{CH}_4$  fluxes remain low ( $\leq 37$   $\text{nmol m}^{-2} \text{s}^{-1}$ ). As WTL rises from  $-0.7$  to  $0.1$  m, the wetland transits from being very dry to wet and even inundation conditions, resulting in a steady increase in  $\text{CH}_4$  fluxes from  $37$   $\text{nmol m}^{-2} \text{s}^{-1}$  (corresponding to WTL of  $-0.7$  m) to  $150$   $\text{nmol m}^{-2} \text{s}^{-1}$  (WTL of  $0.1$  m). However, as WTL continues to rise to  $0.3$  m,  $\text{CH}_4$  fluxes decrease to  $125$   $\text{nmol m}^{-2} \text{s}^{-1}$ , before rising again to around  $150$   $\text{nmol m}^{-2} \text{s}^{-1}$  at WTL of  $0.6$  m or higher.

Figures 2f and 2g illustrate the individual impacts of  $T_{\text{air}}$  and WTL on wetland  $\text{CH}_4$  emissions, respectively, while Figure 2h demonstrates their combined effects. It shows that subtropical freshwater wetland  $\text{CH}_4$  fluxes generally increase with both  $T_{\text{air}}$  and WTL. Moreover, it highlights the synergistic effects of  $T_{\text{air}}$  and WTL: when WTL is below  $-0.7$  m,  $T_{\text{air}}$  has minimal impact on  $\text{CH}_4$  fluxes; when WTL ranges from  $-0.7$  and  $0.1$  m,  $\text{CH}_4$  fluxes only increase with  $T_{\text{air}}$  when it exceeds 24°C; however, when WTL surpasses  $0.1$  m,  $\text{CH}_4$  fluxes become more responsive to changes in  $T_{\text{air}}$ , particularly when  $T_{\text{air}}$  rises above 24°C.

Additionally, we used SHAP (SHapley Additive exPlanations) values to identify and quantify key variables influencing subtropical freshwater wetland methane fluxes (Text S3 in Supporting Information S1 and Figure S9 in Supporting Information S2). These results are consistent with the findings obtained from Gini importance values, as demonstrated here.

### 3.3. Regional Estimations of Subtropical Freshwater Wetland $\text{CH}_4$ Emissions

The upscaled climatological mean of subtropical freshwater wetland  $\text{CH}_4$  emissions, at a high spatial resolution of  $0.0083^\circ \times 0.0083^\circ$  ( $\sim 1$  km  $\times$  1 km) and weighted by the National Wetlands Inventory (NWI) freshwater wetland percentage per pixel (following Equation 3), revealed that  $\text{CH}_4$  emissions from the SE US subtropical freshwater wetlands ranged from 0 to  $163.06$   $\text{nmol m}^{-2} \text{s}^{-1}$  during 1982–2010. Intense  $\text{CH}_4$  fluxes ( $>30$   $\text{nmol CH}_4 \text{ m}^{-2} \text{s}^{-1}$ ) were notably present in the coastal areas, the Everglades, the Mobile-Tensaw River Delta, and the Mississippi Delta (Figure 3a), consistent with the dense distribution of wetland ecosystems within these regions (Figure 1). The variability in  $\text{CH}_4$  fluxes (Figure 3b) closely follows the climatological mean (Figure 3a), with high emission hotspots corresponding to areas of high variability. The unweighted and the Wetland Area and Dynamics for Methane Modeling (WAD2M)-weighted (Z. Zhang et al., 2021) climatological means and variability of monthly

**Figure 2.** Random forest (RF) model estimated (y-axis) versus measured (x-axis) monthly mean wetland  $\text{CH}_4$  fluxes for sites: (a) US-DPW, (b) US-LA2, (c) US-MAC, and (d) US-NC4. The black line is the 1:1 line, and the red line is the best-fit line between the simulated and measured wetland  $\text{CH}_4$  fluxes.  $R^2$  represents the coefficient of determination, while MAE denotes the mean absolute error (unit:  $\text{nmol m}^{-2} \text{s}^{-1}$ ). (e) Variable importance analysis in the RF model based on Gini importance values. The x-axis lists explanatory variables ranked in descending order of importance: air temperature ( $T_{\text{air}}$ ), water level (WTL), wind speed (WS), fall (Fall), incoming shortwave radiation (SW\_IN), vapor pressure deficit (VPD), summer (Summer), precipitation (P), spring (Spring), and winter (Winter). The y-axis shows the relative importance of these variables in estimating wetland methane fluxes. Partial dependence of wetland  $\text{CH}_4$  fluxes (y-axis) on dominant predictors (x-axis), (f)  $T_{\text{air}}$ , (g) WTL, and (h)  $T_{\text{air}}$  and WTL combined. The dots in (f–h) are eddy covariance tower measurements from the four FLUXNET- $\text{CH}_4$  sites.

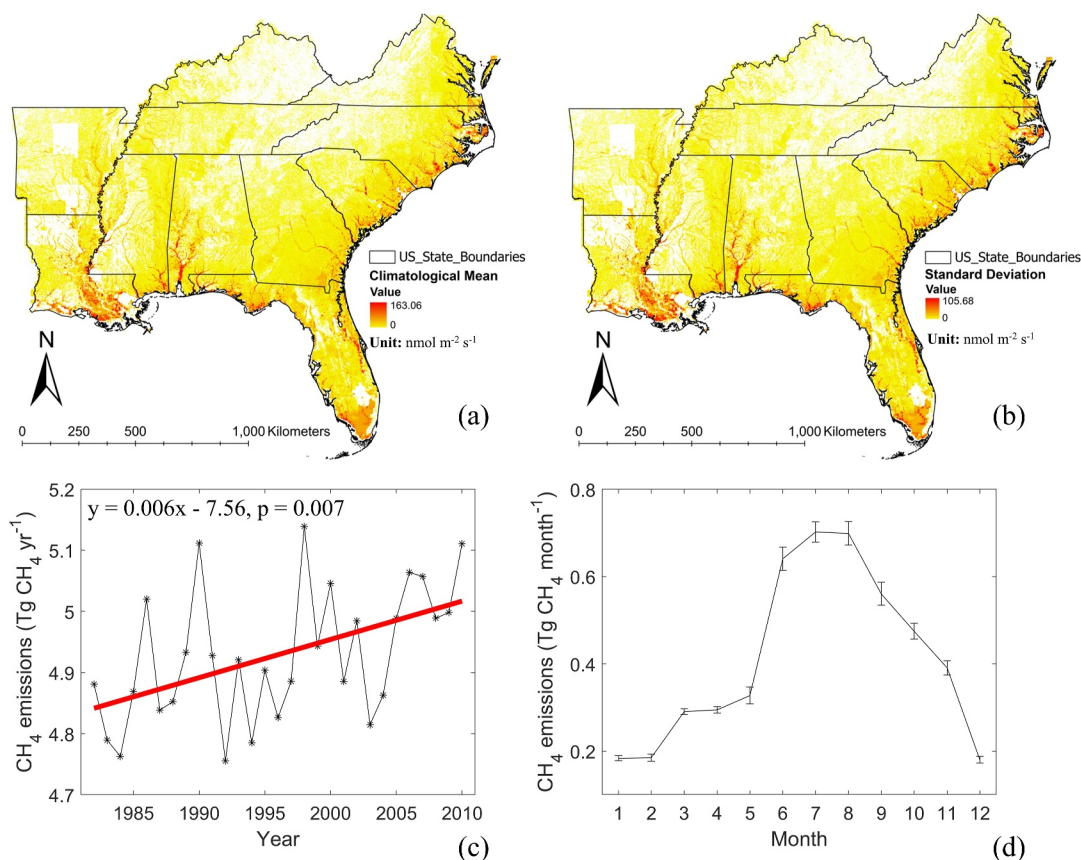


**Figure 3.** (a) Climatological mean and (b) variability of subtropical freshwater wetland CH<sub>4</sub> emissions. CH<sub>4</sub> flux variability in (b) was calculated as one standard deviation of the monthly CH<sub>4</sub> emissions across subtropical freshwater wetlands in the SE US during 1982–2010 at a high spatial resolution of  $0.0083^\circ \times 0.0083^\circ$  ( $\sim 1 \text{ km} \times 1 \text{ km}$ ). These estimates were generated using the RF regression model and based on the NWI freshwater wetland percentage data. (c) Interannual and (d) monthly variations of CH<sub>4</sub> emissions from SE US subtropical freshwater wetlands. The red line in (c) represents the best-fit linear regression line between the simulated CH<sub>4</sub> emissions and the year. The bars in (d) indicate one standard deviation of monthly emissions during 1982–2010.

subtropical freshwater wetland CH<sub>4</sub> emissions are present in Figures S10 and S11 in Supporting Information S2, respectively, showing similar patterns to the NWI-weighted CH<sub>4</sub> emissions depicted in Figures 3a and 3b.

On an inter-annual scale, annual CH<sub>4</sub> emissions from subtropical freshwater wetland ecosystems in the SE US exhibited substantial variability (Figure 3c). The annual mean CH<sub>4</sub> emission was approximately  $4.93 \pm 0.11 \text{ Tg CH}_4 \text{ yr}^{-1}$ , ranging from  $4.76 \text{ Tg CH}_4 \text{ yr}^{-1}$  in 1992 to  $5.14 \text{ Tg CH}_4 \text{ yr}^{-1}$  in 1998. This variability was strongly correlated with the variations in  $T_{\text{air}}$ , with a correlation coefficient ( $r$ ) of 0.92 ( $p = 1.92 \times 10^{-5}$ , Figure S12a in Supporting Information S2). Conversely, the variability in annual WTL had a lesser impact on annual CH<sub>4</sub> emissions ( $p = 0.259$ ). Furthermore, an increasing trend ( $p = 0.007$ ) in annual subtropical freshwater wetland CH<sub>4</sub> emissions was detected from 1982 to 2010 (Figure 3c), indicating an increase of  $\sim 0.006 \text{ Tg CH}_4 \text{ yr}^{-1}$  since 1982.

The monthly mean CH<sub>4</sub> emissions from subtropical freshwater wetland ecosystems in the SE US exhibited a clear seasonal pattern, with weak emissions occurring from December through February and strong emissions observed in June, July, and August. The highest CH<sub>4</sub> emission occurred in July ( $0.70 \text{ Tg CH}_4 \text{ month}^{-1}$ ), while the lowest occurred in December ( $0.18 \text{ Tg CH}_4 \text{ month}^{-1}$ ) (Figure 3d). This seasonal disparity was primarily driven by differences in  $T_{\text{air}}$  between winter and summer. In summer, the average  $T_{\text{air}}$  across the region was approximately  $25^\circ\text{C}$  (Figure S12b in Supporting Information S2), resulting in high CH<sub>4</sub> fluxes ( $\sim 116 \text{ nmol m}^{-2} \text{ s}^{-1}$ , Figure 2f), whereas  $T_{\text{air}}$  dropped to around  $8^\circ\text{C}$  during winter (Figure S12b in Supporting Information S2), leading to much

lower CH<sub>4</sub> fluxes ( $\sim 51 \text{ nmol m}^{-2} \text{ s}^{-1}$ , Figure 2f). A transitional period with a lower emission plateau was observed from March to May, followed by a sharp increase in June.

Interestingly, the variability in monthly wetland CH<sub>4</sub> emissions also differed seasonally. The standard deviations of monthly wetland CH<sub>4</sub> emissions were higher during summer months (June, July, August, and September) and lower in winter months (December, January, and February) (Figure 3d). These phenomena can be attributed to the sigmoidal relationship between wetland methane fluxes and T<sub>air</sub>: CH<sub>4</sub> fluxes were more sensitive to T<sub>air</sub> within the range of 24–28°C. While the standard deviations of T<sub>air</sub> in summer were only 0.84°C, smaller than those in winter (1.92°C, Figure S12b in Supporting Information S2), even slight fluctuations in T<sub>air</sub> around 25°C could cause disproportionate changes in CH<sub>4</sub> emissions during the summer months. In contrast, changes in CH<sub>4</sub> emissions were relatively minor when T<sub>air</sub> ranged from 4°C to 10°C during the winter months (Figure 2f).

### 3.4. Comparison of Regional Subtropical Freshwater Wetland CH<sub>4</sub> Flux Estimates

To further evaluate the regional subtropical freshwater wetland CH<sub>4</sub> fluxes (1982–2010) estimated from the RF regression model in Section 3.3, we compared them with the CH<sub>4</sub> fluxes derived from the “Wetlands” sector of the top-down CMS Methane Flux for North America (only available for 2010 and 2011, Turner et al., 2015) for the overlapping year 2010 (Figure 4) and the bottom-up Global Wetland Methane Emissions derived from FLUXNET and the UpCH<sub>4</sub> Model (UpCH<sub>4</sub>, McNicol et al., 2023) for their overlapping period 2001–2010 (Figure S13 in Supporting Information S2). As the CMS Methane Flux and UpCH<sub>4</sub> products have spatial resolutions of  $0.5^\circ \times 0.667^\circ$  and  $0.25^\circ \times 0.25^\circ$ , respectively, the RF regression model estimated subtropical freshwater wetland CH<sub>4</sub> fluxes ( $0.0083^\circ \times 0.0083^\circ$ ) were first resampled to  $0.5^\circ \times 0.667^\circ$  and  $0.25^\circ \times 0.25^\circ$  to match the spatial resolution of the CMS Methane Flux and UpCH<sub>4</sub> products before comparison, respectively. This was achieved using the “Resample” function (Resampling Technique: NEAREST) within the “Data Management” Tool in ArcMap 10.5.1 (ArcGIS, 2016).

Linear regressions between the RF regression model estimates and those derived from the “Wetlands” sector of the CMS Methane Flux product within each  $0.5^\circ \times 0.667^\circ$  grid closely approached the 1:1 line on both monthly and annual scales, with R<sup>2</sup> values of 0.39 and 0.48 ( $p < 0.0001$ ) and MAE values of  $7.02 \text{ nmol m}^{-2} \text{ s}^{-1}$  and  $5.91 \text{ nmol m}^{-2} \text{ s}^{-1}$ , respectively (Figures 4a and 4c). Additionally, we compared the distributions of the RF-simulated and the CMS Methane Flux product-derived CH<sub>4</sub> fluxes on monthly and annual scales in 2010 (Figures 4b and 4d). Statistically, there was no significant difference between the CMS Methane Flux product-derived and RF regression model-estimated wetland CH<sub>4</sub> fluxes, with paired p-values of 0.42 and 0.13 at the monthly and annual scales, separately. Furthermore, our spatial correlation analysis demonstrated significant positive correlations between the two data sets (Figure 4e). Collectively, these results suggest good consistency between the wetland CH<sub>4</sub> fluxes estimated by our RF regression model and those derived from the “Wetlands” sector of the CMS Methane Flux product on regional scales.

Comparison results of our developed subtropical freshwater wetland CH<sub>4</sub> flux estimates over the SE US against the bottom-up UpCH<sub>4</sub>-WAD2M product (UpCH<sub>4</sub> weighted by the Wetland Area and Dynamics for Methane Modeling (WAD2M) (Z. Zhang et al., 2021)) can be found in Text S4 in Supporting Information S1.

## 4. Discussion

### 4.1. Development of Random Forest Regression Models Using FLUXNET-CH<sub>4</sub> Measurements

In this study, we developed RF regression models using measurements from four FLUXNET-CH<sub>4</sub> wetland sites to estimate subtropical freshwater wetland CH<sub>4</sub> fluxes across the Southeastern United States from 1982 to 2010. We acknowledge the relatively small number of EC sites used in our model development. Some previous studies on upscaling wetland CH<sub>4</sub> or CO<sub>2</sub> fluxes incorporated chamber-based flux measurements collected from the literature (e.g., Huang et al., 2021; Yuan et al., 2024; Zhu et al., 2013; Zou et al., 2022). However, quite large discrepancies have been documented between chamber-based and EC measurements of wetland CH<sub>4</sub> emissions (Deshmukh et al., 2023; Krauss et al., 2016; Meijide et al., 2011). For example, Krauss et al. (2016) reported that chamber-measured wetland CH<sub>4</sub> fluxes were 2–4 times higher than EC fluxes measured at about the same location. Such differences stem from the dramatically different spatial footprint of EC towers (a radius of the order of hundreds to thousands of meters) and chambers (a sub-meter radius or side length), as well as the timing

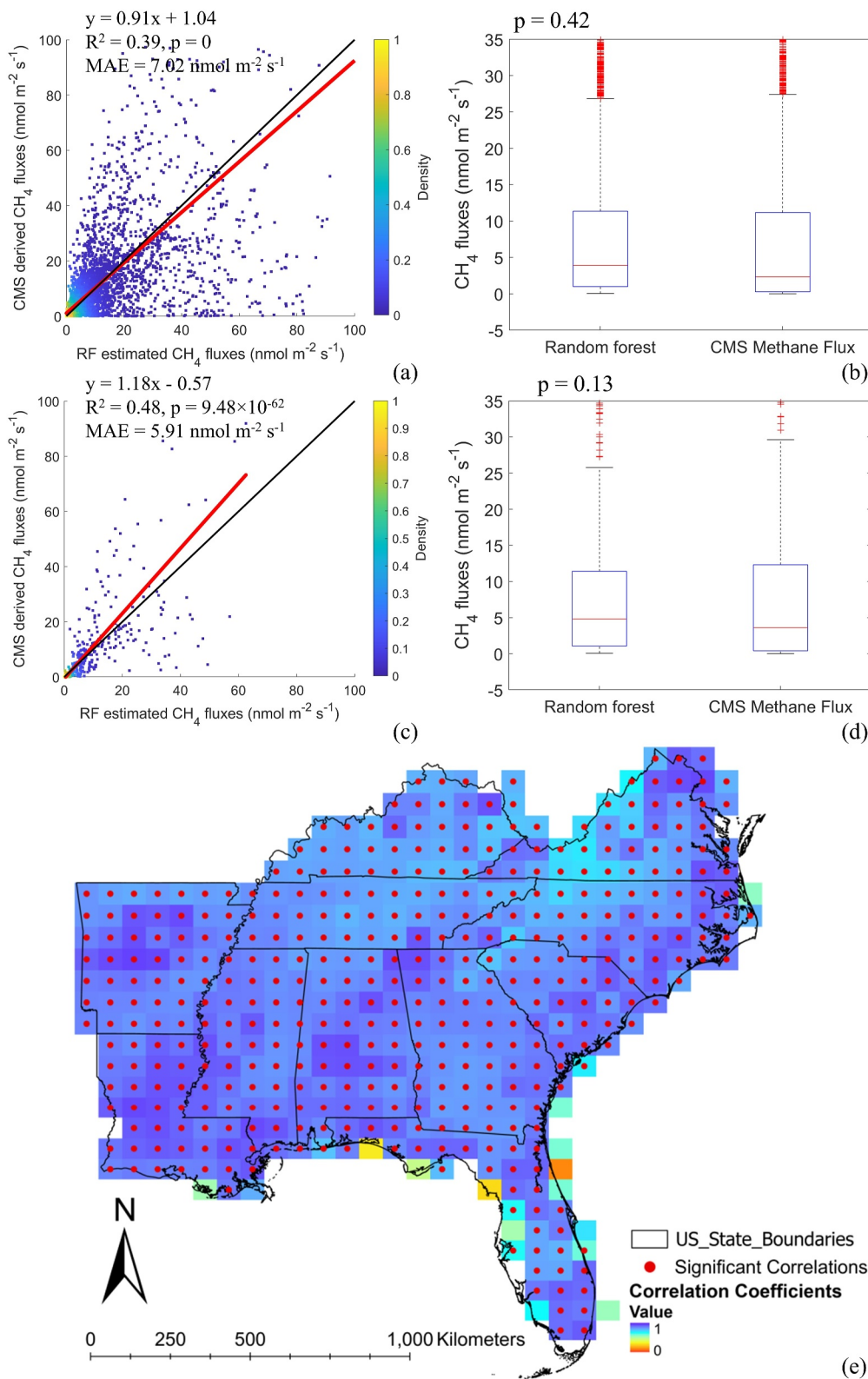


Figure 4.

of the data collection (EC towers record measurements every 30 min, 48 times per day, while chambers typically collect during daytime when CH<sub>4</sub> fluxes are inherently higher).

We also sought to enhance our data set for model development by collecting field-measured wetland CH<sub>4</sub> flux data (most measured by chambers) within the SE US through literature searches on the Web of Science (<https://www.webofscience.com/wos/woscc/basic-search>). However, large differences were found between chamber-based wetland CH<sub>4</sub> flux measurements and those from the FLUXNET-CH<sub>4</sub> product, our RF regression model estimates, the top-down CMS Methane Flux product, and the bottom-up UpCH<sub>4</sub> product (not shown). Therefore, we decided not to incorporate chamber-based wetland CH<sub>4</sub> flux measurements. Instead, we used all publicly available EC measurements (3,105 site-days) within freshwater wetland ecosystems in the SE US.

To assess the representativeness of the four FLUXNET-CH<sub>4</sub> sites, we conducted a principal component analysis (PCA), comparing environmental variables across all 0.0083° × 0.0083° grids with those at the four EC sites (Figure S14a in Supporting Information S2). While the sites do not capture all environmental variability, they cluster within the central PCA feature space, overlapping substantially with the broader regional environmental distribution. Additionally, we mapped the four EC sites onto a two-dimensional feature space of key environmental variables—T<sub>air</sub> and WTL—for all 0.0083° × 0.0083° wetland grid cells (Figure S14b in Supporting Information S2). The T<sub>air</sub> and WTL at these EC sites span critical ranges of T<sub>air</sub> (10–30°C) and WTL (–1.5–0.7 m), capturing key thresholds for CH<sub>4</sub> fluxes, particularly T<sub>air</sub> between 24 and 28°C and WTL between –0.7 and 0.1 m. This extensive coverage enables us to employ a time-for-space substitution approach, utilizing the 3,105 site-day measurements from the four sites as representative samples for the entire SE US. This representativeness is further supported by the site constituency representativeness analysis illustrated in Figure S12 of McNicol et al. (2023).

Despite the limited number of EC sites in our study, these sites feature long-term continuous CH<sub>4</sub> flux measurements and represent predominant subtropical freshwater wetland types in the SE US, including freshwater forested/shrub wetlands (US-NC4) and freshwater emergent wetlands (US-DPW, US-LA2, and US-MAC). Our RF regression models demonstrated strong performance across all four sites, achieving an average R<sup>2</sup> of 0.67 during leave-one-group-out cross-validation (LOGOCV) at the monthly scale (Figures 2a–2d). This satisfactory performance underscores the broad regional applicability of our RF regression model for subtropical freshwater wetlands in the SE US.

In summary, it is reasonable to extrapolate the RF regression model developed using all available EC data to estimate subtropical freshwater wetland CH<sub>4</sub> fluxes over the entire SE US. This approach, utilizing several representative sites to characterize a region with relatively homogeneous hydroclimatic conditions, offers a viable strategy for addressing the global wetland methane budget, particularly given the limited number of EC sites available worldwide. When additional in situ EC sites are available, future studies should incorporate them into the analysis to further enhance the model's representativeness of the SE US.

#### 4.2. Environmental Predictors of Subtropical Freshwater Wetland Methane Emissions

This study examined 14 potential explanatory variables affecting subtropical freshwater wetland CH<sub>4</sub> emissions in the SE US. These predictors reflect the impacts of climate (T<sub>air</sub>, P, VPD, SW\_IN, WS, LE, and H), hydrology (WTL), vegetation (LAI, fAPAR, GPP, and NEE), and seasonality (season) on wetland CH<sub>4</sub> fluxes. Consequently, including SW\_IN, VPD, T<sub>air</sub>, P, WS, WTL, and season as predictors resulted in the best-performing RF model, exhibiting a performance (R<sup>2</sup> = 0.67) comparable to previous studies using ML models to estimate wetland methane emissions (e.g., Huang et al., 2021; McNicol et al., 2023; Peltola et al., 2019). Our study's appreciable R<sup>2</sup> between the simulated and measured wetland CH<sub>4</sub> fluxes demonstrated that the RF regression model effectively captured the relationship between environmental variables and subtropical freshwater wetland CH<sub>4</sub> fluxes, providing an accurate estimation of these emissions. Among the environmental predictors examined,

**Figure 4.** Linear regressions between the CMS Methane Flux product-derived and the RF regression model-estimated subtropical freshwater wetland CH<sub>4</sub> fluxes on (a) monthly and (c) annual scales in 2010. The black line is the 1:1 line, while the red line is the best-fit line. Boxplots of paired *t*-test results comparing the CMS Methane Flux product-derived and the RF regression model-estimated CH<sub>4</sub> fluxes at the (b) monthly and (d) annual scales in 2010. The red solid horizontal line, box, and whisker ends indicate the median, 25th and 75th percentiles, and the 10th and 90th percentiles, respectively. The data points outside the ranges are shown by the red plus (+) sign. (e) Spatial correlations between the CMS Methane Flux product-derived and the RF regression model-estimated wetland CH<sub>4</sub> fluxes on a monthly scale in 2010. Significant correlations at the 5% significance level are stippled.

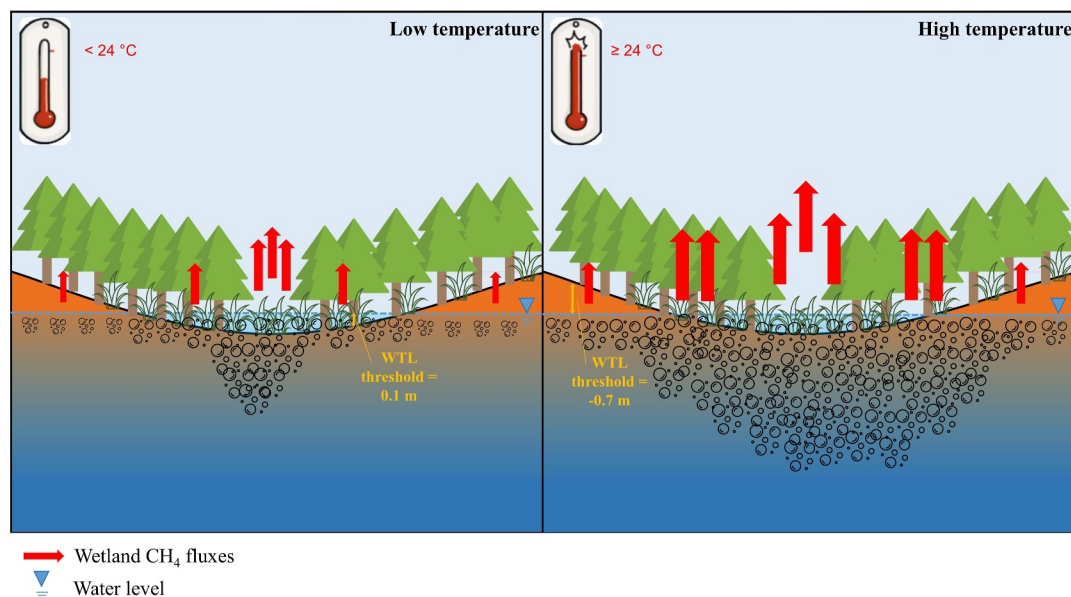


**Figure 5.** Conceptual model illustrating the effects of air temperature ( $T_{\text{air}}$ ) and water level (WTL) on methane emissions in subtropical freshwater wetlands. Under the same WTL conditions, (left panel) lower temperatures (below the lower bound of the critical  $T_{\text{air}}$  range, which is  $24^{\circ}\text{C}$ ) result in less wetland  $\text{CH}_4$  emissions compared to (right panel) higher temperatures. Within each panel, once WTL surpasses the WTL threshold (0.1 m in low-temperature conditions and  $-0.7$  m in high-temperature conditions), wetland  $\text{CH}_4$  emissions increase (indicated by more and larger bubbles and red arrows) along the gradients of WTL.

$T_{\text{air}}$  and WTL emerged as the most important predictors in estimating methane fluxes from the SE US subtropical freshwater wetlands (Figure 2e).

#### 4.2.1. Temperature Effects on Subtropical Freshwater Wetland Methane Emissions

Temperature has been widely recognized as a significant factor influencing  $\text{CH}_4$  fluxes across a range of temperate and boreal wetland ecosystems (Bridgman & Richardson, 1992; McNicol et al., 2023; Turetsky et al., 2014; Yvon-Durocher et al., 2014; Zhu et al., 2013). The positive relationship between wetland  $\text{CH}_4$  fluxes and  $T_{\text{air}}$  detected in this study (Figures 2f and 5) is expected due to the stimulation of microbial activity by higher temperature without water limitation (Keller et al., 2023; Knox et al., 2021; Yvon-Durocher et al., 2014), aligning with both laboratory studies (e.g., Whalen & Reeburgh, 1996) and field observations (e.g., Bellisario et al., 1999; Christensen et al., 2003). Furthermore, the critical temperature range of  $24\text{--}28^{\circ}\text{C}$  identified in this study (Figure 2f) is consistent with the optimal temperature for methanogens documented in previous research (Deng et al., 2019; Metje & Frenzel, 2005; Nozhevnikova et al., 2001).

The relationship between temperature and wetland  $\text{CH}_4$  emissions explains the observed interannual variability (Figure 3c) and seasonal (summer vs. winter) differences (Figure 3d) in wetland  $\text{CH}_4$  emissions across the SE US. With increasing trends ( $p < 0.05$ ) in the number of days experiencing air temperatures exceeding the lower threshold ( $24^{\circ}\text{C}$ ) of the critical temperature range (Figure S12c in Supporting Information S2), wetlands in the SE US are poised to experience substantial boosts in  $\text{CH}_4$  emissions due to the disproportionate enhancement of wetland  $\text{CH}_4$  emissions once air temperatures surpass  $24^{\circ}\text{C}$ .

Although  $T_{\text{air}}$  also affects methane oxidation (Segers, 1998; Z. Wang et al., 1996; L. Zhang et al., 2020), its effects on methanogenesis outperform those on methane oxidation at the studied sites, leading to an increase in net  $\text{CH}_4$  emissions with rising temperature, as shown in Figure 2f. This is consistent with the findings of Dunfield et al. (1993) and Le Mer and Roger (2001).

We acknowledged that soil temperature may exert a more direct and immediate influence on wetland methane emissions compared with air temperature (Hanis et al., 2013; Rinne et al., 2018; Yuan et al., 2022). While soil temperature can diverge from air temperature in certain situations (Watts, 1975), air temperature and surface soil

temperature are generally well correlated. Additionally, it is essential to note that comprehensive soil temperature data are not consistently accessible across all FLUXNET-CH<sub>4</sub> sites. In cases where such data are available, variations in measurement depth may exist (Chang et al., 2021).

#### 4.2.2. Water Level Effects on Subtropical Freshwater Wetland Methane Emissions

Subtropical freshwater wetlands experience fluctuations in water levels (WTL) throughout the year (Davidson et al., 2012). These fluctuations regulate redox conditions within the soil column, thereby controlling methanogenesis (Bridgham & Richardson, 1992; Goodrich et al., 2015; Huang et al., 2021; Ise et al., 2008; Olefeldt et al., 2017). Higher WTL leads to prolonged inundation, which prevents oxygen from reaching the wetland substrate and maintains anaerobic conditions that facilitate CH<sub>4</sub> production (Bansal et al., 2018; Gao et al., 2014; Oertel et al., 2016; Smith et al., 2003). Conversely, lower WTL allows oxygen to penetrate the substrate, creating aerobic conditions that suppress methanogenesis and simultaneously enhance CH<sub>4</sub> oxidation due to increased oxygen availability in the overlying zones above WTL (Olefeldt et al., 2017; J. Yang et al., 2013). Our findings support these mechanisms, showing elevated wetland methane fluxes during high WTL periods (WTL > 0.1 m) and consistently low fluxes during low WTL periods (WTL < -0.7 m) (Figures 2g and 5).

WTL dynamics are affected by precipitation, which is modulated by climate variability and changes (Murguia-Flores et al., 2023; van der Valk, 2012). Future projections indicate more intense and frequent rainfall extremes in the SE US (Kunkel et al., 2013), potentially leading to increased flooding events and significant methane hotspots. Moreover, human activities can modify WTL dynamics. For example, lowering WTL in managed wetlands has been shown to reduce CH<sub>4</sub> emissions. Evans et al. (2021) observed a significant reduction in CH<sub>4</sub> emissions with each 10 cm decrease in WTL in peatlands drained for agriculture. Therefore, optimal management practices for natural wetlands should prioritize maintaining appropriate WTL.

#### 4.2.3. Combined Effects of Temperature and Water Levels on Subtropical Freshwater Wetland Methane Emissions

In tropical regions, where temperature is generally not a limiting factor due to consistently high  $T_{\text{air}}$  and minimal year-round variations (Murguia-Flores et al., 2023), several studies have highlighted the importance of water levels (WTL) as the primary determinant of methane emissions in tropical wetlands (Bloom et al., 2012; Z. Zhang et al., 2017). For example, Luta et al. (2021) demonstrated that fluctuations in WTL at the soil-water interface regulate CH<sub>4</sub> emissions in a tropical peatland in Malaysia. In contrast, in temperate and boreal regions, WTL does not appear as an important predictor as it often remains above the surface or exhibits small variations (Song et al., 2011; Strachan et al., 2015; Yuan et al., 2024). Instead, temperature is emphasized as the primary determinant of methane emissions in these high-latitude regions, as evidenced by Yuan et al. (2024), who showed that temperature primarily governs the trend and variability of CH<sub>4</sub> emissions in the Boreal-Arctic region. However, in subtropical regions such as the SE US, our study reveals that CH<sub>4</sub> emissions from freshwater wetlands are sensitive to variations in both  $T_{\text{air}}$  and WTL (Figures 2e–2h and 5), differentiating them from their high-latitude and tropical counterparts. This underscores the priority of refining CH<sub>4</sub> emission responses to  $T_{\text{air}}$  and WTL processes in bottom-up models tailored to different climatic zones.

In subtropical freshwater wetlands,  $T_{\text{air}}$  and WTL collectively regulate methane emissions. The combined effects of  $T_{\text{air}}$  and WTL on wetland CH<sub>4</sub> emissions (Figure 2h) illustrate that the response of CH<sub>4</sub> emissions to variations in WTL depends on  $T_{\text{air}}$  conditions, and vice versa. Concentrating exclusively on the impact of either  $T_{\text{air}}$  or WTL on wetland CH<sub>4</sub> emissions might result in an incomplete comprehension of wetland CH<sub>4</sub> emissions. For instance, at  $T_{\text{air}}$  below 24°C, it might be inferred that the threshold for WTL is around 0.1 m above the land surface, below which CH<sub>4</sub> emissions are consistently low. However, when  $T_{\text{air}}$  exceeds 24°C, the WTL threshold shifts to approximately 0.7 m below the land surface, representing a huge deviation from low-temperature conditions. This temperature-dependent shift in WTL thresholds and their impact on CH<sub>4</sub> emissions is consistently supported by observational data across all sites (Figure S15 in Supporting Information S2). Additionally, we observed an unexpected drop in methane emissions when the WTL ranged from 0.1 to 0.3 m (Figure 2g). This decline is not a result of increased WTL but rather stems from the average temperatures associated with this WTL range being lower than those corresponding to WTL between 0 and 0.1 m, based on the EC flux measurements from the four sites used to develop the RF regression model (Figure S16 in Supporting Information S2). Since these average

temperatures fall within or near the critical ranges of  $T_{\text{air}}$  (24–28°C), the lower  $T_{\text{air}}$  results in much weaker  $\text{CH}_4$  fluxes, even at higher WTL.

The synergistic effects of  $T_{\text{air}}$  and WTL on wetland  $\text{CH}_4$  emissions also elucidate the low emission plateau during March and May observed in the seasonal cycle of  $\text{CH}_4$  emissions from SE US wetlands (Figure 3d). If we solely consider the impact of  $T_{\text{air}}$  on  $\text{CH}_4$  emissions, we would expect  $\text{CH}_4$  fluxes to increase continuously from spring to summer as  $T_{\text{air}}$  rises (Figure S12b in Supporting Information S2). However, there is a noticeable plateau in  $\text{CH}_4$  emissions during March and May (Figure 3d). This plateau is primarily influenced by low WTL during these months. When WTL is lower than the critical WTL threshold of 0.1 m (corresponding to  $T_{\text{air}}$  below 24°C), the sensitivity of  $\text{CH}_4$  fluxes to  $T_{\text{air}}$  diminishes, resulting in reduced  $\text{CH}_4$  emissions despite rising  $T_{\text{air}}$ . However, the limitation on  $\text{CH}_4$  fluxes due to WTL is only evident when  $T_{\text{air}}$  is below the critical threshold of 24°C. Once  $T_{\text{air}}$  exceeds 24°C, as in June, although WTL remains low—similar to levels in April and May—and is above the critical threshold of  $-0.7$  m (corresponding to  $T_{\text{air}}$  is above 24°C),  $\text{CH}_4$  emissions boost. This interplay between  $T_{\text{air}}$  and WTL aligns with seasonal wetland  $\text{CH}_4$  flux patterns observed at most eddy-covariance flux tower sites (Text S5 in Supporting Information S1), emphasizing the critical role of both factors in regulating  $\text{CH}_4$  emissions.

Besides the benefit of a more comprehensive view of wetland  $\text{CH}_4$  emissions, understanding the combined impact of  $T_{\text{air}}$  and WTL helps refine the regional upscaling of wetland  $\text{CH}_4$  emissions, especially in subtropical regions such as the SE US. The comparison of the monthly time series of our wetland  $\text{CH}_4$  emission estimates with those from UpCH4-WAD2M (Figure S13d in Supporting Information S2) indicates some discrepancies between the two data sets. One reason for these discrepancies is that most sites used in McNicol et al. (2023) are located in high-latitude regions. Given the significant spatial variability in how wetland methane emissions respond to temperature across climatic zones—showing a declining trend in favorable temperatures from low to high latitudes (Bohdalkova et al., 2014; Inglett et al., 2012; Turetsky et al., 2014)—the optimal  $T_{\text{air}}$  detected in McNicol et al. (2023), approximately 10°C (Figure S6c in McNicol et al., 2023), is considerably lower than the critical threshold of 24°C found in our study. Thus, the model trained by McNicol et al. (2023) is skewed toward high-latitude regions and may not be suitable for subtropical regions. Another reason contributing to the discrepancy lies in the omission of WTL as a predictor in their model. As demonstrated in our study, WTL is a significant limiting factor for wetland  $\text{CH}_4$  emissions (Figure 2h). Without incorporating WTL, the upscaling model may overestimate wetland  $\text{CH}_4$  emissions, particularly in areas where WTL is substantially below the land surface. We recognize the limited availability of WTL measurements at EC tower sites. In such cases, additional hydrological variables highly correlated with WTL should be considered, such as soil water content and certain drought indices (e.g., Palmer Drought Severity Index).

#### 4.2.4. Limitations in Temporal Lags and Missing Predictors

Although the RF regression model demonstrated reasonable performance with an average  $R^2$  value of 0.67 between the monthly mean wetland  $\text{CH}_4$  fluxes estimated by the model and the actual measurements at testing sites, it is important to acknowledge that this analysis did not account for temporal lags between environmental variables and  $\text{CH}_4$  fluxes, nor did it encompass all potential drivers responsible for inter- and intra-site variability in wetland  $\text{CH}_4$  emissions. As a result, the model failed to account for all sources of variability within the data.

For example, recent flux synthesis using EC data sets (e.g., Knox et al., 2021) highlights GPP as a dominant predictor of  $\text{CH}_4$  emissions. However, the inclusion of GPP as an explanatory variable in our RF model did not improve model performance, and the relative importance of GPP was low. This could be attributed to the fact that our model did not account for the temporal lags between environmental variables and  $\text{CH}_4$  fluxes. Previous studies have shown that  $\text{CH}_4$  fluxes typically lag behind GPP by  $\sim 13 \pm 23$  days, reflecting the time required for labile organic carbon inputs from plants—such as exudates or fresh detritus—to be processed into  $\text{CH}_4$  emissions (Knox et al., 2021; Megonigal et al., 2004). Future studies could explore the use of deep learning models, such as Long Short-Term Memory (LSTM) neural networks, which are adept at learning and capturing temporal dependencies, to improve  $\text{CH}_4$  upscaling.

Additional environmental variables, such as soil properties (e.g., pH, phenolics, total nitrogen, organic carbon content, ferric iron concentration, and the availability of substrates), may also influence wetland  $\text{CH}_4$  emissions (Cheng et al., 2021; Christensen et al., 2003; Gutenberg et al., 2019; Huang et al., 2021; Laanbroek, 2010; Peltola et al., 2019; Richardson et al., 2023; Sutton-Grier & Megonigal, 2011; H. Wang et al., 2015, 2021; Yvon-Durocher et al., 2014; Zhu et al., 2013). For example, studies (Gutenberg et al., 2019; Richardson et al., 2023;

H. Wang et al., 2015, 2021) have shown that methane emissions from pocosins (wetland bogs with peat soil and woody shrubs) are negligible due to high phenolic concentrations in the pocosin soils, which inhibit CH<sub>4</sub> emissions (Miao et al., 2012; Ward et al., 2013; Ye et al., 2012). However, none of the four sites analyzed in this study are located in pocosins with deep peats (Table 1). Thus, the RF regression model developed in this study may not account for the inhibitory effects of phenolics on wetland CH<sub>4</sub> emissions, potentially leading to an overestimation of CH<sub>4</sub> emissions from pocosins.

Additionally, soil properties such as substrate availability, the iron cycle, and soil pH are also suggested to impact CH<sub>4</sub> production (Christensen et al., 2003; DeLaune et al., 1986; Laanbroek, 2010). However, the spatial distributions of these variables are either unavailable or only available as static data sets, such as those provided by the Soil Survey Geographic Database (SSURGO) and the International Soil Reference and Information Centre-World Inventory of Soil Emission Potentials (ISRIC-WISE). Incorporating these static soil variables into the RF regression model did not improve the performance of the model or even degrade it (not shown). Nonetheless, it is worthwhile for future studies to investigate the impact of soil properties on regulating wetland CH<sub>4</sub> emissions as more soil properties are surveyed and dynamic soil data become available.

### 4.3. Increasing Trends in Annual Subtropical Freshwater Wetland Methane Emissions

From 1982 to 2010, annual methane fluxes from SE US subtropical freshwater wetlands exhibited an increasing trend, with emissions rising by ~0.006 Tg CH<sub>4</sub> per year ( $p = 0.007$ , Figure 3c). This trend, based on the static NWI wetland area, underscores the critical role of temperature increases in driving methane emissions. A strong positive correlation ( $r = 0.92$ ,  $p = 1.92 \times 10^{-5}$ ; Figure S12a in Supporting Information S2) highlights how elevated temperatures stimulate microbial methanogenesis in anaerobic wetland soils (Bridgman et al., 2013; Turetsky et al., 2014). A similar increasing trend was observed in the UpCH<sub>4</sub>-WAD2M flux product, which incorporates dynamic wetland areas from the WAD2M data set (Figure S20 in Supporting Information S2). Notably, this trend is strongly correlated with an increase in wetland areas identified by WAD2M ( $r = 0.56$ ,  $p = 0.016$ ), suggesting that wetland expansion has also contributed to rising methane emissions.

The dual influence of temperature and wetland area dynamics highlights the complexity of methane flux trends in the SE US. Climate warming will likely continue to enhance methane emissions by stimulating microbial activity and by expanding wetland inundation due to altered precipitation regimes (Z. Zhang et al., 2021). However, localized factors, such as urbanization and sea-level rise, may lead to wetland loss and potentially offset these trends locally (Nicholls & Cazenave, 2010).

To better understand and predict wetland CH<sub>4</sub> emissions, future studies should prioritize developing high-resolution, long-term, dynamic wetland maps and disentangling the relative contributions of wetland area changes and climate variability. Investigating the impacts of wetland management and restoration on methane flux trends under future climate scenarios will also be critical. Such integrated analyses will enhance our understanding of regional and global wetland CH<sub>4</sub> budgets and inform strategies for effective climate mitigation.

### 4.4. Uncertainties in Regional CH<sub>4</sub> Flux Estimates

Despite the satisfactory agreement between the RF regression model estimated and the top-down (CMS Methane Flux) and bottom-up (UpCH<sub>4</sub>) model-derived monthly average wetland CH<sub>4</sub> fluxes shown in Section 3.4, some uncertainties persist in estimating subtropical freshwater wetland methane emissions. The main uncertainty may arise from the wetland extent and gridded water level data used in regional-scale estimates (Zhu et al., 2011, 2013). In this study, both fixed and dynamic wetland percentages for each grid were employed based on the NWI and the WAD2M data sets, respectively. For the estimation of subtropical freshwater wetland CH<sub>4</sub> emissions weighted by NWI over the SE US during 1982–2010, wetland degradation/migration/conversion/expansion over the years was not taken into account. As a result, our estimates of methane emissions may be overestimated for wetlands experiencing degradation, while they may be underestimated for expanding wetland areas (He et al., 2022; White et al., 2021). Meanwhile, for the estimation of wetland CH<sub>4</sub> emissions weighted by WAD2M over the SE US during 2000–2010, although WAD2M incorporates temporal variations in wetland areas, its spatial resolution is considerably coarser ( $0.25^\circ \times 0.25^\circ$ ), and it only covers data back to the year 2000. Furthermore, the total freshwater wetland areas estimated by the NWI are nearly three times larger than those estimated by WAD2M across the SE US (Figure S21 in Supporting Information S2), highlighting the uncertainty associated with the total emissions attributed to the chosen wetland map.

To explore the impact of WTL uncertainty on CH<sub>4</sub> flux estimates, we compared in situ daily WTL measurements from 61 monitoring wells within freshwater wetlands to model-simulated WTL data from de Graaf et al. (2019). The comparison yielded a median correlation coefficient ( $r$ ) of 0.39 and a median mean error of  $-1.24$  m (Figure S22 in Supporting Information S2), reflecting reasonable agreement with previous studies (e.g., Bolaños Chavarría et al., 2022; Reinecke et al., 2020). To quantify the effect of this uncertainty, we added 1.24 m to the simulated WTL (“WTL+1.24 m” scenario) and re-estimated CH<sub>4</sub> emissions for the SE US. Weighted by NMI freshwater wetland percentage, emissions under the “WTL+1.24 m” scenario were consistently higher than those under the original WTL scenario, with regional-scale median interannual and monthly percentage differences of 10.6% and 9.7%, respectively (Figure S23 in Supporting Information S2). Despite discrepancies, to the best of our knowledge, the monthly gridded WTL product developed by de Graaf et al. (2019) remains the best available high-resolution ( $0.083^\circ \times 0.083^\circ$ ) spatial WTL data set for CH<sub>4</sub> modeling. This highlights the critical need for more accurate, long-term, and high-spatial-resolution water level data to improve CH<sub>4</sub> flux estimates and reduce uncertainties.

## 5. Conclusions

Based on FLUXNET-CH<sub>4</sub> flux measurements from wetlands and associated climatic, hydrological, and seasonality data, we developed random forest regression models to understand how environmental variables affect CH<sub>4</sub> emissions from subtropical freshwater wetlands and further created the first high-spatial-resolution ( $0.0083^\circ \times 0.0083^\circ$ , approximately 1 km  $\times$  1 km at the Equator) and long-term (29 years from 1982 to 2010) gridded CH<sub>4</sub> flux product for subtropical freshwater wetlands in the Southeastern (SE) United States (US).

CH<sub>4</sub> emissions from subtropical freshwater wetlands are particularly sensitive to variations in both air temperature ( $T_{\text{air}}$ ) and water levels (WTL), different from high-latitude peatlands (sensitive to  $T_{\text{air}}$ ) and tropical wetlands (sensitive to WTL). Understanding the synergistic effects of  $T_{\text{air}}$  and WTL on methane emissions from subtropical freshwater wetlands not only helps refine the regional and global upscaling of wetland CH<sub>4</sub> emissions but also deepens our comprehension of the mechanisms behind these emissions.

Our high-spatial-resolution CH<sub>4</sub> flux estimates for subtropical freshwater wetlands in the SE US exhibit strong agreement with the top-down Carbon Monitoring System methane product and the bottom-up UpCH<sub>4</sub> estimates, confirming their reliability. The climatological mean of monthly CH<sub>4</sub> emissions from subtropical freshwater wetlands displayed large spatial variability, varying from 0 to 163.06 nmol m<sup>-2</sup> s<sup>-1</sup>, with coastal areas, the Mississippi Delta, the Mobile-Tensaw River Delta, and the Everglades being predominant sources. The annual mean CH<sub>4</sub> emission from SE US freshwater wetlands was estimated to be  $4.93 \pm 0.11$  Tg CH<sub>4</sub> yr<sup>-1</sup>, ranging from 4.76 Tg CH<sub>4</sub> yr<sup>-1</sup> in 1992 to 5.14 Tg CH<sub>4</sub> yr<sup>-1</sup> in 1998. Our analysis also revealed a distinct seasonal pattern, with weaker emissions from December to February, contrasted by stronger emissions from June to August.

The high spatial resolution ( $\sim 1$  km  $\times$  1 km) achieved in this study marks a notable advancement over existing upscaled CH<sub>4</sub> flux products. This fine resolution provides a more detailed representation of spatial variability in methane emissions, capturing heterogeneities often lost in coarser-scale products. It also enables the identification of CH<sub>4</sub> emission hotspots that may be obscured at coarser scales, facilitating more targeted monitoring and mitigation efforts. By offering granular insights into the spatial dynamics and variability of CH<sub>4</sub> emissions, this product serves as a valuable constraint for estimating subtropical freshwater wetland methane emissions in the SE US. Additionally, it supports the validation and parameterization of highly uncertain biogeochemical processes associated with wetland CH<sub>4</sub> emissions in bottom-up process-based models, paving the way for future CH<sub>4</sub> flux upscaling studies in the SE US. Furthermore, the upscaled data set provides improved prior information for top-down transport inversion models, enabling a more dependable differentiation between natural and anthropogenic effects on atmospheric CH<sub>4</sub> concentrations.

## Data Availability Statement

Flux tower measurements, climate data, vegetation indices, wind speed, water level, remotely sensed CH<sub>4</sub> product, and static and dynamic wetland maps were sourced from the FLUXNET-CH<sub>4</sub> Community Product (<https://fluxnet.org/data/fluxnet-ch4-community-product/>), the Daymet data set ([https://daac.orl.gov/cgi-bin/dsvviewer.pl?ds\\_id=2129](https://daac.orl.gov/cgi-bin/dsvviewer.pl?ds_id=2129)), NOAA Climate Data Record (<https://www.ncei.noaa.gov/access/metadata/landing-page/bin/iso?id=gov.noaa.ncdc:C00898>), NOAA Physical Sciences Laboratory (<https://psl.noaa.gov/data/>

gridded/data.livneh.html), de Graaf et al. (2019), Carbon Monitoring System Project ([https://disc.gsfc.nasa.gov/datasets/CMS\\_CH4\\_FLX\\_NAD\\_1/summary](https://disc.gsfc.nasa.gov/datasets/CMS_CH4_FLX_NAD_1/summary)), National Wetlands Inventory (<https://fwsprimary.wim.usgs.gov/wetlands/apps/wetlands-mapper/>), and Wetland Area and Dynamics for Methane Modeling (WAD2M, <https://zenodo.org/records/3998454>), respectively. The high-spatial-resolution ( $0.0083^\circ \times 0.0083^\circ$ ) and long-term (1982–2010) gridded wetland CH<sub>4</sub> flux product for the Southeastern United States developed in our study are available via ZENODO (<https://zenodo.org/records/14602319>; He & Li, 2025).

#### Acknowledgments

The US-NC4 flux tower project was supported by USDA NIFA (Multi-agency A.5 Carbon Cycle Science Program) award 2014-67003-22068, DOE NICCR award 08-SC-NICCR-1072, USDA Forest Service awards 13-JV-11330110-081 and 21-JV-11330180-52, and DOE LBNL award M2100680. J. King designed and created the US-NC4 field site with both J. King and M. Aguilos actively involved in the maintenance of the US-NC4 field site. de Graaf acknowledges funding from the European Union (ERC Starting Grant, GROW-10104110).

#### References

- Aguilos, M., Mitra, B., Noormets, A., Minick, K., Prajapati, P., Gavazzi, M., et al. (2020). Long-term carbon flux and balance in managed and natural coastal forested wetlands of the Southeastern USA. *Agricultural and Forest Meteorology*, 288, 108022. <https://doi.org/10.1016/j.agrformet.2020.108022>
- Aguilos, M., Warr, I., Irving, M., Gregg, O., Grady, S., Peele, T., et al. (2022). The unabated atmospheric carbon losses in a drowning wetland forest of North Carolina: A point of no return? *Forests*, 13(8), 1264. <https://doi.org/10.3390/f13081264>
- Altman, N., & Krzywinski, M. (2017). Ensemble methods: Bagging and random forests. *Nature Methods*, 14(10), 933–935. <https://doi.org/10.1038/nmeth.4438>
- Andersen, R., Chapman, S. J., & Artz, R. R. E. (2013). Microbial communities in natural and disturbed peatlands: A review. *Soil Biology and Biochemistry*, 57, 979–994. <https://doi.org/10.1016/j.soilbio.2012.10.003>
- Andronova, N. G., & Karol, I. L. (1993). The contribution of USSR sources to global methane emission. *Chemosphere*, 26(1–4), 111–126. [https://doi.org/10.1016/0045-6535\(93\)90416-3](https://doi.org/10.1016/0045-6535(93)90416-3)
- ArcGIS. Version 10.5.1. (2016). *ArcGIS. Version 10.5.1*. Environmental Systems Research Institute, Inc.
- Baldocchi, D. (2014). Measuring fluxes of trace gases and energy between ecosystems and the atmosphere—the state and future of the eddy covariance method. *Global Change Biology*, 20(12), 3600–3609. <https://doi.org/10.1111/gcb.12649>
- Baldocchi, D., Falge, E., Gu, L., Olson, R., Hollinger, D., Running, S., et al. (2001). FLUXNET: A new tool to study the temporal and spatial variability of ecosystem-scale carbon dioxide, water vapor, and energy flux densities. *Bulletin of the American Meteorological Society*, 82(11), 2415–2434. [https://doi.org/10.1175/1520-0477\(2001\)082<2415:FANTTS>2.3.CO;2](https://doi.org/10.1175/1520-0477(2001)082<2415:FANTTS>2.3.CO;2)
- Bansal, S., Tangen, B., & Finocchiaro, R. (2018). Diurnal patterns of methane flux from a seasonal wetland: Mechanisms and methodology. *Wetlands*, 38(5), 933–943. <https://doi.org/10.1007/s13157-018-1042-5>
- Bartlett, K. B., & Harriss, R. C. (1993). Review and assessment of methane emissions from wetlands. *Chemosphere*, 26(1–4), 261–320. [https://doi.org/10.1016/0045-6535\(93\)90427-7](https://doi.org/10.1016/0045-6535(93)90427-7)
- Beck, H. E., McVicar, T. R., Vergopolan, N., Berg, A., Lutsko, N. J., Dufour, A., et al. (2023). High-resolution (1 km) Köppen-Geiger maps for 1901–2099 based on constrained CMIP6 projections. *Scientific Data*, 10(1), 724. <https://doi.org/10.1038/s41597-023-02549-6>
- Beck, H. E., Zimmermann, N. E., McVicar, T. R., Vergopolan, N., Berg, A., & Wood, E. F. (2018). Present and future Köppen-Geiger climate classification maps at 1-km resolution. *Scientific Data*, 5(1), 1–12. <https://doi.org/10.1038/sdata.2018.214>
- Beer, C., Reichstein, M., Tomelleri, E., Ciais, P., Jung, M., Carvalhais, N., et al. (2010). Terrestrial gross carbon dioxide uptake: Global distribution and covariation with climate. *Science*, 329(5993), 834–838. <https://doi.org/10.1126/science.1184984>
- Bellisario, L. M., Bubier, J. L., Moore, T. R., & Chanton, J. P. (1999). Controls on CH<sub>4</sub> emissions from a northern peatland. *Global Biogeochemical Cycles*, 13(1), 81–91. <https://doi.org/10.1029/1998GB900021>
- Bloom, A. A., Bowman, K. W., Lee, M., Turner, A. J., Schroeder, R., Worden, J. R., et al. (2017). A global wetland methane emissions and uncertainty dataset for atmospheric chemical transport models (WetCHARTs version 1.0). *Geoscientific Model Development*, 10(6), 2141–2156. <https://doi.org/10.5194/gmd-10-2141-2017>
- Bloom, A. A., Palmer, P. I., Fraser, A., & Reay, D. S. (2012). Seasonal variability of tropical wetland CH<sub>4</sub> emissions: The role of the methanogen-available carbon pool. *Biogeosciences*, 9(8), 2821–2830. <https://doi.org/10.5194/bg-9-2821-2012>
- Bloom, A. A., Palmer, P. I., Fraser, A., Reay, D. S., & Frankenberg, C. (2010). Large-scale controls of methanogenesis inferred from methane and gravity spaceborne data. *Science*, 327(5963), 322–325. <https://doi.org/10.1126/science.1175176>
- Bodesheim, P., Jung, W., Gans, F., Mahecha, M. D., & Reichstein, M. (2018). Upscaled diurnal cycles of land-atmosphere fluxes: A new global half-hourly data product. *Earth System Science Data*, 10(3), 1327–1365. <https://doi.org/10.5194/essd-10-1327-2018>
- Bohdalkova, L., Novak, M., Buzek, F., Kreisinger, J., Bindler, R., Pazderu, K., & Pacheroova, P. (2014). The response of a mid-and high latitude peat bog to predicted climate change: Methane production in a 12-month peat incubation. *Mitigation and Adaptation Strategies for Global Change*, 19(7), 997–1010. <https://doi.org/10.1007/s11027-013-9456-0>
- Bolaños Chavarría, S., Werner, M., Salazar, J. F., & Betancur Vargas, T. (2022). Benchmarking global hydrological and land surface models against GRACE in a medium-size tropical basin. *Hydrology and Earth System Sciences*, 26(16), 4323–4344. <https://doi.org/10.5194/hess-26-4323-2022>
- Breiman, L. (2001). Random forests. *Machine Learning*, 45(1), 5–32. <https://doi.org/10.1023/A:1010933404324>
- Bridgman, S. D., Cadillo-Quiroz, H., Keller, J. K., & Zhuang, Q. (2013). Methane emissions from wetlands: Biogeochemical, microbial, and modeling perspectives from local to global scales. *Global Change Biology*, 19(5), 1325–1346. <https://doi.org/10.1111/gcb.12131>
- Bridgman, S. D., & Richardson, C. J. (1992). Mechanisms controlling soil respiration (CO<sub>2</sub> and CH<sub>4</sub>) in southern peatlands. *Soil Biology and Biochemistry*, 24(11), 1089–1099. [https://doi.org/10.1016/0038-0717\(92\)90058-6](https://doi.org/10.1016/0038-0717(92)90058-6)
- Cao, M., Marshall, S., & Gregson, K. (1996). Global carbon exchange and methane emissions from natural wetlands: Application of a process-based model. *Journal of Geophysical Research*, 101(D9), 14399–14414. <https://doi.org/10.1029/96JD00219>
- Chang, K. Y., Riley, W. J., Brodie, E. L., McCalley, C. K., Crill, P. M., & Grant, R. F. (2019). Methane production pathway regulated proximally by substrate availability and distally by temperature in a high-latitude mire complex. *Journal of Geophysical Research: Biogeosciences*, 124(10), 3057–3074. <https://doi.org/10.1029/2019JG005355>
- Chang, K. Y., Riley, W. J., Crill, P. M., Grant, R. F., & Saleska, S. R. (2020). Hysteretic temperature sensitivity of wetland CH<sub>4</sub> fluxes explained by substrate availability and microbial activity. *Biogeosciences*, 17(22), 5849–5860. <https://doi.org/10.5194/bg-17-5849-2020>
- Chang, K. Y., Riley, W. J., Knox, S. H., Jackson, R. B., McNicol, G., Poulter, B., et al. (2021). Substantial hysteresis in emergent temperature sensitivity of global wetland CH<sub>4</sub> emissions. *Nature Communications*, 12(1), 2266. <https://doi.org/10.1038/s41467-021-22452-1>

- Chen, W., Zhang, F., Wang, B., Wang, J., Tian, D., Han, G., et al. (2019). Diel and seasonal dynamics of ecosystem-scale methane flux and their determinants in an alpine meadow. *Journal of Geophysical Research: Biogeosciences*, *124*(6), 1731–1745. <https://doi.org/10.1029/2019jg005011>
- Cheng, S., Qin, C., Xie, H., Wang, W., Hu, Z., Liang, S., & Feng, K. (2021). A new insight on the effects of iron oxides and dissimilated metal-reducing bacteria on CH<sub>4</sub> emissions in constructed wetland matrix systems. *Bioresource Technology*, *320*, 124296. <https://doi.org/10.1016/j.biortech.2020.124296>
- Christensen, T. R., Ekberg, A., Ström, L., Mastepanov, M., Panikov, N., Öquist, M., et al. (2003). Factors controlling large scale variations in methane emissions from wetlands. *Geophysical Research Letters*, *30*(7). <https://doi.org/10.1029/2002GL016848>
- Chu, H., Luo, X., Ouyang, Z., Chan, W. S., Dengel, S., Biraud, S. C., et al. (2021). Representativeness of Eddy-Covariance flux footprints for areas surrounding AmeriFlux sites. *Agricultural and Forest Meteorology*, *301*, 108350. <https://doi.org/10.1016/j.agrformet.2021.108350>
- Dahl, T. E. (2011). *Status and trends of wetlands in the conterminous United States 2004 to 2009*. US Department of the Interior, US Fish and Wildlife Service, Fisheries and Habitat Conservation. Retrieved from <https://www.fws.gov/wetlands/documents/status-and-trends-of-wetlands-in-the-conterminous-united-states-2004-to-2009.pdf>
- Dahl, T. E., & Stedman, S. M. (2013). *Status and trends of wetlands in the coastal watersheds of the Conterminous United States 2004 to 2009*. US Department of the Interior, US Fish and Wildlife Service, Fisheries and Habitat Conservation. Retrieved from <https://www.fws.gov/wetlands/documents/status-and-trends-of-wetlands-in-the-coastal-watersheds-of-the-conterminous-us-2004-to-2009.pdf>
- Dai, Z., Trettin, C. C., Li, C., Li, H., Sun, G., & Amartya, D. M. (2012). Effect of assessment scale on spatial and temporal variations in CH<sub>4</sub>, CO<sub>2</sub>, and N<sub>2</sub>O fluxes in a forested wetland. *Water, Air, & Soil Pollution*, *223*(1), 253–265. <https://doi.org/10.1007/s11270-011-0855-0>
- Davidson, T. A., Mackay, A. W., Wolski, P., Mazebedi, R., Murray-Hudson, M. I. K. E., & Todd, M. (2012). Seasonal and spatial hydrological variability drives aquatic biodiversity in a flood-pulsed, sub-tropical wetland. *Freshwater Biology*, *57*(6), 1253–1265. <https://doi.org/10.1111/j.1365-2427.2012.02795.x>
- Davis, M. J. (2010). Contrast coding in multiple regression analysis: Strengths, weaknesses, and utility of popular coding structures. *Journal of Data Science*, *8*(1), 61–73. [https://doi.org/10.6339/JDS.2010.08\(1\).563](https://doi.org/10.6339/JDS.2010.08(1).563)
- de Graaf, I. E., Gleeson, T., Van Beek, L. P. H., Sutanudjaja, E. H., & Bierkens, M. F. (2019). Environmental flow limits to global groundwater pumping. *Nature*, *574*(7776), 90–94. <https://doi.org/10.1038/s41586-019-1594-4>
- DeLaune, R. D., Smith, C. J., & Patrick Jr, W. H. (1986). Methane production in Mississippi River deltaic plain peat. *Organic Geochemistry*, *9*(4), 193–197. [https://doi.org/10.1016/0146-6380\(86\)90069-0](https://doi.org/10.1016/0146-6380(86)90069-0)
- Delwiche, K. B., Knox, S. H., Malhotra, A., Fluet-Chouinard, E., McNicol, G., Feron, S., et al. (2021). FLUXNET-CH4: A global, multi-ecosystem dataset and analysis of methane seasonality from freshwater wetlands. *Earth System Science Data*, *13*(7), 3607–3689. <https://doi.org/10.5194/essd-13-3607-2021>
- Deng, Y., Liu, P., & Conrad, R. (2019). Effect of temperature on the microbial community responsible for methane production in alkaline NamCo wetland soil. *Soil Biology and Biochemistry*, *132*, 69–79. <https://doi.org/10.1016/j.soilbio.2019.01.024>
- Dengel, S., Zona, D., Sachs, T., Aurela, M., Jammet, M., Parmentier, F. J. W., et al. (2013). Testing the applicability of neural networks as a gap-filling method using CH<sub>4</sub> flux data from high latitude wetlands. *Biogeosciences*, *10*(12), 8185–8200. <https://doi.org/10.5194/bg-10-8185-2013>
- Deshmukh, C. S., Susanto, A. P., Nardi, N., Nurholis, N., Kurnianto, S., Suardiwerianto, Y., et al. (2023). Net greenhouse gas balance of fibre wood plantation on peat in Indonesia. *Nature*, *616*(7958), 1–7. <https://doi.org/10.1038/s41586-023-05860-9>
- Dunfield, P., Dumont, R., & Moore, T. R. (1993). Methane production and consumption in temperate and subarctic peat soils: Response to temperature and pH. *Soil Biology and Biochemistry*, *25*(3), 321–326. [https://doi.org/10.1016/0038-0717\(93\)90130-4](https://doi.org/10.1016/0038-0717(93)90130-4)
- Evans, C. D., Peacock, M., Baird, A. J., Artz, R. R. E., Burden, A., Callaghan, N., et al. (2021). Overriding water table control on managed peatland greenhouse gas emissions. *Nature*, *593*(7860), 548–552. <https://doi.org/10.1038/s41586-021-03523-1>
- Friberg, T., Christensen, T. R., & Sjøgaard, H. (1997). Rapid response of greenhouse gas emission to early spring thaw in a subarctic mire as shown by micrometeorological techniques. *Geophysical Research Letters*, *24*(23), 3061–3064. <https://doi.org/10.1029/97GL03024>
- Friedman, J. H. (2001). Greedy function approximation: A gradient boosting machine. *Annals of Statistics*, *29*(5), 1189–1232. <https://doi.org/10.1214/aos/1013203451>
- Gao, B., Ju, X., Su, F., Meng, Q., Oenema, O., Christie, P., et al. (2014). Nitrous oxide and methane emissions from optimized and alternative cereal cropping systems on the North China plain: A two-year field study. *Science of the Total Environment*, *472*, 112–124. <https://doi.org/10.1016/j.scitotenv.2013.11.003>
- Goodrich, J. P., Campbell, D. I., Roulet, N. T., Clearwater, M. J., & Schipper, L. A. (2015). Overriding control of methane flux temporal variability by water table dynamics in a Southern Hemisphere, raised bog. *Journal of Geophysical Research: Biogeosciences*, *120*(5), 819–831. <https://doi.org/10.1002/2014JG002844>
- Gutenberg, L., Krauss, K. W., Qu, J. J., Ahn, C., Hogan, D., Zhu, Z., & Xu, C. (2019). Carbon dioxide emissions and methane flux from forested wetland soils of the Great Dismal Swamp, USA. *Environmental Management*, *64*(2), 190–200. <https://doi.org/10.1007/s00267-019-01177-4>
- Hanis, K. L., Tenuta, M., Amiro, B. D., & Papakyriakou, T. N. (2013). Seasonal dynamics of methane emissions from a subarctic fen in the Hudson Bay Lowlands. *Biogeosciences*, *10*(7), 4465–4479. <https://doi.org/10.5194/bg-10-4465-2013>
- Hastie, T. J., Tibshirani, R. J., & Friedman, J. H. (2001). *The elements of statistical learning: Data mining, inference, and prediction*. Springer.
- He, K., & Li, W. (2025). High-spatial-resolution (0.0083° × 0.0083°) and long-term (1982 to 2010) monthly gridded wetland CH<sub>4</sub> flux product for the Southeastern United States [Dataset]. <https://doi.org/10.5281/zenodo.14602319>
- He, K., Li, W., Zhang, Y., Sun, G., McNulty, S. G., Flanagan, N. E., & Richardson, C. J. (2023). Identifying driving hydrogeomorphic factors of coastal wetland downgrading using random forest classification models. *Science of the Total Environment*, *894*, 164995. <https://doi.org/10.1016/j.scitotenv.2023.164995>
- He, K., Zhang, Y., Li, W., Sun, G., & McNulty, S. (2022). Detecting coastal wetland degradation by combining remote sensing and hydrologic modeling. *Forests*, *13*(3), 411. <https://doi.org/10.3390/f13030411>
- Hefner, J. M., Wilen, B. O., Dahl, T. E., & Frayer, W. E. (1994). *Southeast wetlands; status and trends, Mid1970's to Mid-1980's*. US Department of the Interior, Fish and Wildlife Service. Retrieved from <https://www.fws.gov/wetlands/Documents%5CSoutheast-Wetlands-Status-and-Trends-mid-1970s-to-mid-1980s.pdf>
- Hinkle, C. R., & Bracho, R. (2020). FLUXNET-CH4 US-DPW disney wilderness preserve wetland [Dataset]. <https://doi.org/10.18140/FLX/1669672>
- Holm, G. O., Perez, B. C., McWhorter, D. E., Krauss, K. W., Raynie, R. C., & Killebrew, C. J. (2020). FLUXNETCH4 US-LA2 Salvador WMA freshwater marsh [Dataset]. <https://doi.org/10.18140/FLX/1669681>
- Huang, Y., Ciaisi, P., Luo, Y., Zhu, D., Wang, Y., Qiu, C., et al. (2021). Tradeoff of CO<sub>2</sub> and CH<sub>4</sub> emissions from global peatlands under water-table drawdown. *Nature Climate Change*, *11*(7), 618–622. <https://doi.org/10.1038/s41558-021-01059-w>

- Inglett, K. S., Inglett, P. W., Reddy, K. R., & Osborne, T. Z. (2012). Temperature sensitivity of greenhouse gas production in wetland soils of different vegetation. *Biogeochemistry*, *108*(1–3), 77–90. <https://doi.org/10.1007/s10533-011-9573-3>
- IPCC. (2021). In V. Masson-Delmotte, P. Zhai, A. Pirani, S. L. Connors, C. Péan, S. Berger, et al. (Eds.), *Climate Change 2021: The Physical Science Basis. Contribution of Working Group I to the Sixth Assessment Report of the Intergovernmental Panel on Climate Change*. Cambridge University Press.
- Ise, T., Dunn, A. L., Wofsy, S. C., & Moorcroft, P. R. (2008). High sensitivity of peat decomposition to climate change through water-table feedback. *Nature Geoscience*, *1*(11), 763–766. <https://doi.org/10.1038/ngeo331>
- Jung, M., Reichstein, M., Ciais, P., Seneviratne, S. I., Sheffield, J., Goulden, M. L., et al. (2010). Recent decline in the global land evapotranspiration trend due to limited moisture supply. *Nature*, *467*(7318), 951–954. <https://doi.org/10.1038/nature09396>
- Jung, M., Reichstein, M., Margolis, H. A., Cescatti, A., Richardson, A. D., Arain, M. A., et al. (2011). Global patterns of land-atmosphere fluxes of carbon dioxide, latent heat, and sensible heat derived from eddy covariance, satellite, and meteorological observations. *Journal of Geophysical Research*, *116*(G3), G00J07. <https://doi.org/10.1029/2010JG001566>
- Jung, M., Reichstein, M., Schwalm, C. R., Huntingford, C., Sitch, S., Ahlström, A., et al. (2017). Compensatory water effects link yearly global land CO<sub>2</sub> sink changes to temperature. *Nature*, *541*(7638), 516–520. <https://doi.org/10.1038/nature20780>
- Keller, J. K., Bridgman, S. D., Takagi, K. K., Zalman, C. A., Rush, J. E., Anderson, C., et al. (2023). Microbial organic matter reduction regulates methane and carbon dioxide production across an ombrotrophic-minerotrophic peatland gradient. *Soil Biology and Biochemistry*, *182*, 109045. <https://doi.org/10.1016/j.soilbio.2023.109045>
- Knox, S. H., Bansal, S., McNicol, G., Schafer, K., Sturtevant, C., Ueyama, M., et al. (2021). Identifying dominant environmental predictors of freshwater wetland methane fluxes across diurnal to seasonal time scales. *Global Change Biology*, *27*(15), 3582–3604. <https://doi.org/10.1111/gcb.15661>
- Knox, S. H., Jackson, R. B., Poulter, B., McNicol, G., Fluet-Chouinard, E., Zhang, Z., et al. (2019). FLUXNET-CH<sub>4</sub> synthesis activity: Objectives, observations, and future directions. *Bulletin of the American Meteorological Society*, *100*(12), 2607–2632. <https://doi.org/10.1175/BAMS-D-18-0268.1>
- Kottek, M., Grieser, J., Beck, C., Rudolf, B., & Rubel, F. (2006). World Map of the Köppen-Geiger climate classification updated. *Meteorologische Zeitschrift*, *15*(3), 259–263. <https://doi.org/10.1127/0941-2948/2006/0130>
- Krauss, K. W., Holm Jr, G. O., Perez, B. C., McWhorter, D. E., Cormier, N., Moss, R. F., et al. (2016). Component greenhouse gas fluxes and radiative balance from two deltaic marshes in Louisiana: Pairing chamber techniques and eddy covariance. *Journal of Geophysical Research: Biogeosciences*, *121*(6), 1503–1521. <https://doi.org/10.1002/2015JG003224>
- Kriticos, D. J., Webber, B. L., Leriche, A., Ota, N., Macadam, I., Bathols, J., & Scott, J. K. (2012). CliMond: Global high-resolution historical and future scenario climate surfaces for bioclimatic modelling. *Methods in Ecology and Evolution*, *3*(1), 53–64. <https://doi.org/10.1111/j.2041-210X.2011.00134.x>
- Kuhn, M., & Johnson, K. (2013). *Applied predictive modeling* (Vol. 26, p. 13). Springer. <https://doi.org/10.1007/978-1-4614-6849-3>
- Kunkel, K. E., Stevens, L. E., Stevens, S. E., Sun, L., Janssen, E., Wuebbles, D., et al. (2013). Regional climate trends and scenarios for the US National climate Assessment: Part 2. Climate of the Southeast US. Retrieved from <https://repository.library.noaa.gov/view/noaa/56807>
- Laanbroek, H. J. (2010). Methane emission from natural wetlands: Interplay between emergent macrophytes and soil microbial processes. A mini-review. *Annals of Botany*, *105*(1), 141–153. <https://doi.org/10.1093/aob/mcp201>
- Lan, X., Thoning, K. W., & Dlugokencky, E. J. (2024). Trends in globally-averaged CH<sub>4</sub>, N<sub>2</sub>O, and SF<sub>6</sub> determined from NOAA global monitoring laboratory measurements version 2024-04. <https://doi.org/10.15132/P8XG-AA10>
- Lehner, B., Verdin, K., & Jarvis, A. (2008). New global hydrography derived from spaceborne elevation data. *Eos, Transactions American Geophysical Union*, *89*(10), 93–94. <https://doi.org/10.1029/2008EO100001>
- Le Mer, J., & Roger, P. (2001). Production, oxidation, emission and consumption of methane by soils: A review. *European Journal of Soil Biology*, *37*(1), 25–50. [https://doi.org/10.1016/S1164-5563\(01\)01067-6](https://doi.org/10.1016/S1164-5563(01)01067-6)
- Livneh, B., Rosenberg, E. A., Lin, C., Nijssen, B., Mishra, V., Andreadis, K. M., et al. (2013). A long-term hydrologically based dataset of land surface fluxes and states for the conterminous United States: Update and extensions. *Journal of Climate*, *26*(23), 9384–9392. <https://doi.org/10.1175/JCLI-D-12-00508.1>
- Luta, W., Ahmed, O. H., Omar, L., Heng, R. K. J., Choo, L. N. L. K., Jalloh, M. B., et al. (2021). Water table fluctuation and methane emission in pineapples (*Ananas comosus* (L.) Merr.) cultivated on a tropical peatland. *Agronomy*, *11*(8), 1448. <https://doi.org/10.3390/agronomy11081448>
- McNicol, G., Fluet-Chouinard, E., Ouyang, Z., Knox, S., Zhang, Z., Aalto, T., et al. (2023). Upscaling wetland methane emissions from the FLUXNET-CH<sub>4</sub> eddy covariance network (UpCH<sub>4</sub> v1.0): Model development, network assessment, and budget comparison. *AGU Advances*, *4*(5), e2023AV000956. <https://doi.org/10.1029/2023AV000956>
- McNicol, G., Sturtevant, C. S., Knox, S. H., Dronova, I., Baldocchi, D. D., & Silver, W. L. (2017). Effects of seasonality, transport pathway, and spatial structure on greenhouse gas fluxes in a restored wetland. *Global Change Biology*, *23*(7), 2768–2782. <https://doi.org/10.1111/gcb.13580>
- Megonigal, J. P., Hines, M. E., & Visscher, P. T. (2004). Anaerobic metabolism: Linkages to trace gases and aerobic processes. In W. Schlesinger, H. Holland, & K. Turekian (Eds.), *Treatise on Geochemistry* (Vol. 8, pp. 317–424). Elsevier. <https://doi.org/10.1016/b978-0-08-095975-7.00808-1>
- Meijide, A., Manca, G., Goded, I., Magliulo, V., Di Tommasi, P., Seufert, G., & Cescatti, A. (2011). Seasonal trends and environmental controls of methane emissions in a rice paddy field in Northern Italy. *Biogeosciences*, *8*(12), 3809–3821. <https://doi.org/10.5194/bg-8-3809-2011>
- Metje, M., & Frenzel, P. (2005). Effect of temperature on anaerobic ethanol oxidation and methanogenesis in acidic peat from a northern wetland. *Applied and Environmental Microbiology*, *71*(12), 8191–8200. <https://doi.org/10.1128/AEM.71.12.8191-8200.2005>
- Miao, Y., Song, C., Sun, L., Wang, X., Meng, H., & Mao, R. (2012). Growing season methane emission from a boreal peatland in the continuous permafrost zone of Northeast China: Effects of active layer depth and vegetation. *Biogeosciences*, *9*(11), 4455–4464. <https://doi.org/10.5194/bg-9-4455-2012>
- Mohanty, S. R., Bodelier, P. L., & Conrad, R. (2007). Effect of temperature on composition of the methanotrophic community in rice field and forest soil. *FEMS Microbiology Ecology*, *62*(1), 24–31. <https://doi.org/10.1111/j.1574-6941.2007.00370.x>
- Murguía-Flores, F., Jaramillo, V. J., & Gallego-Sala, A. (2023). Assessing methane emissions from tropical wetlands: Uncertainties from natural variability and drivers at the global scale. *Global Biogeochemical Cycles*, *37*(9), e2022GB007601. <https://doi.org/10.1029/2022GB007601>
- Nicholls, R. J., & Cazenave, A. (2010). Sea-level rise and its impact on coastal zones. *Science*, *328*(5985), 1517–1520. <https://doi.org/10.1126/science.1185782>
- Noormets, A., King, J., Mitra, B., Miao, G., Aguilos, M., Minick, K., et al. (2020). FLUXNET-CH<sub>4</sub> US-NC4 NC\_AlligatorRiver [Dataset]. <https://doi.org/10.18140/FLX/1669686>
- Nozhevnikova, A. N., Simankova, M. V., Parshina, S. N., & Kotsyurbenko, O. R. (2001). Temperature characteristics of methanogenic archaea and acetogenic bacteria isolated from cold environments. *Water Science and Technology*, *44*(8), 41–48. <https://doi.org/10.2166/wst.2001.0460>

- Oertel, C., Matschullat, J., Zurba, K., Zimmermann, F., & Erasmi, S. (2016). Greenhouse gas emissions from soils—A review. *Geochemistry*, 76(3), 327–352. <https://doi.org/10.1016/j.chemer.2016.04.002>
- O'Grady, K. E., & Medoff, D. R. (1988). Categorical variables in multiple regression: Some cautions. *Multivariate Behavioral Research*, 23(2), 243–260. [https://doi.org/10.1207/s15327906mbr2302\\_7](https://doi.org/10.1207/s15327906mbr2302_7)
- Olefeldt, D., Euskirchen, E. S., Harden, J., Kane, E., McGuire, A. D., Waldrop, M. P., & Turetsky, M. R. (2017). A decade of boreal rich fen greenhouse gas fluxes in response to natural and experimental water table variability. *Global Change Biology*, 23(6), 2428–2440. <https://doi.org/10.1111/gcb.13612>
- Pastorello, G., Trotta, C., Canfora, E., Chu, H., Christianson, D., Cheah, Y. W., et al. (2020). The FLUXNET2015 dataset and the ONEFlux processing pipeline for eddy covariance data. *Scientific Data*, 7(1), 1–27. <https://doi.org/10.1038/s41597-020-0534-3>
- Pedhazur, E. J., & Kerlinger, F. N. (1982). *Multiple regression in behavioral research*. Holt, Rinehart, and Winston.
- Peel, M. C., Finlayson, B. L., & McMahon, T. A. (2007). Updated world map of the Köppen-Geiger climate classification. *Hydrology and Earth System Sciences*, 11(5), 1633–1644. <https://doi.org/10.5194/hess-11-1633-2007>
- Peltola, O., Hensen, A., Helfter, C., Belevi Marchesini, L., Bosveld, F. C., Van den Bulk, W. C. M., et al. (2014). Evaluating the performance of commonly used gas analysers for methane eddy covariance flux measurements: The InGOS inter-comparison field experiment. *Biogeosciences*, 11(12), 3163–3186. <https://doi.org/10.5194/bg-11-3163-2014>
- Peltola, O., Vesala, T., Gao, Y., Rätty, O., Alekseychik, P., Aurela, M., et al. (2019). Monthly gridded data product of northern wetland methane emissions based on upscaling eddy covariance observations. *Earth System Science Data*, 11(3), 1263–1289. <https://doi.org/10.5194/essd-11-1263-2019>
- Prasad, A. M., Iverson, L. R., & Liaw, A. (2006). Newer classification and regression tree techniques: Bagging and random forests for ecological prediction. *Ecosystems*, 9(2), 181–199. <https://doi.org/10.1007/s10021-005-0054-1>
- Reddy, K. R., & DeLaune, R. D. (2008). *Biogeochemistry of wetlands science and applications*. CRC Press.
- Reinecke, R., Wachholz, A., Mehl, S., Foglia, L., Niemann, C., & Döhl, P. (2020). Importance of spatial resolution in global groundwater modeling. *Groundwater Series*, 58(3), 363–376. <https://doi.org/10.1111/gwat.12996>
- Richardson, C. J., Flanagan, N. E., & Ho, M. (2023). The effects of hydrologic restoration on carbon budgets and GHG fluxes in southeastern US coastal shrub bogs. *Ecological Engineering*, 194, 107011. <https://doi.org/10.1016/j.ecoleng.2023.107011>
- Richardson, C. J., Flanagan, N. E., Wang, H., & Ho, M. (2022). Annual carbon sequestration and loss rates under altered hydrology and fire regimes in southeastern USA pocosin peatlands. *Global Change Biology*, 28(21), 6370–6384. <https://doi.org/10.1111/gcb.16366>
- Rinne, J., Tuittila, E. S., Peltola, O., Li, X., Raivonen, M., Alekseychik, P., et al. (2018). Temporal variation of ecosystem scale methane emission from a boreal fen in relation to temperature, water table position, and carbon dioxide fluxes. *Global Biogeochemical Cycles*, 32(7), 1087–1106. <https://doi.org/10.1029/2017GB005747>
- Roberts, D. R., Bahn, V., Ciuti, S., Boyce, M. S., Elith, J., Guiller-Arroita, G., et al. (2017). Cross-validation strategies for data with temporal, spatial, hierarchical, or phylogenetic structure. *Ecography*, 40(8), 913–929. <https://doi.org/10.1111/ecog.02881>
- Sanches, L. F., Guenet, B., Marinho, C. C., Barros, N., & de Assis Esteves, F. (2019). Global regulation of methane emission from natural lakes. *Scientific Reports*, 9(1), 255. <https://doi.org/10.1038/s41598-018-36519-5>
- Saunio, M., Bousquet, P., Poulter, B., Peregon, A., Ciais, P., Canadell, J. G., et al. (2017). Variability and quasi-decadal changes in the methane budget over the period 2000–2012. *Atmospheric Chemistry and Physics*, 17(18), 11135–11161. <https://doi.org/10.5194/acp-17-11135-2017>
- Saunio, M., Stavert, A. R., Poulter, B., Bousquet, P., Canadell, J. G., Jackson, R. B., et al. (2020). The global methane budget 2000–2017. *Earth System Science Data*, 12(3), 1561–1623. <https://doi.org/10.5194/essd-12-1561-2020>
- Savi, F., Di Bene, C., Canfora, L., Mondini, C., & Fares, S. (2016). Environmental and biological controls on CH<sub>4</sub> exchange over an evergreen Mediterranean forest. *Agricultural and Forest Meteorology*, 226, 67–79. <https://doi.org/10.1016/j.agrformet.2016.05.014>
- Schuerch, M., Spencer, T., Temmerman, S., Kirwan, M. L., Wolff, C., Lincke, D., et al. (2018). Future response of global coastal wetlands to sea-level rise. *Nature*, 561(7722), 231–234. <https://doi.org/10.1038/s41586-018-0476-5>
- Segers, R. (1998). Methane production and methane consumption: A review of processes underlying wetland methane fluxes. *Biogeochemistry*, 41(1), 23–51. <https://doi.org/10.1023/A:1005929032764>
- Smith, K. A., Ball, T., Conen, F., Dobbie, K. E., Massheder, J., & Rey, A. (2003). Exchange of greenhouse gases between soil and atmosphere: Interactions of soil physical factors and biological processes. *European Journal of Soil Science*, 54(4), 779–791. <https://doi.org/10.1046/j.1351-0754.2003.0567.x>
- Song, C., Sun, L., Huang, Y., Wang, Y., & Wan, Z. (2011). Carbon exchange in a freshwater marsh in the Sanjiang Plain, northeastern China. *Agricultural and Forest Meteorology*, 151(8), 1131–1138. <https://doi.org/10.1016/j.agrformet.2011.04.001>
- Sparks, J. P. (2020). FLUXNET-CH4 US-MAC MacArthur agro-ecology [Dataset]. <https://doi.org/10.18140/FLX/1669683>
- Strachan, I. B., Nugent, K. A., Crombie, S., & Bonneville, M. C. (2015). Carbon dioxide and methane exchange at a cool-temperate freshwater marsh. *Environmental Research Letters*, 10(6), 065006. <https://doi.org/10.1088/1748-9326/10/6/065006>
- Sturtevant, C., Ruddell, B. L., Knox, S. H., Verfaillie, J., Matthes, J. H., Oikawa, P. Y., & Baldocchi, D. (2016). Identifying scale-emergent, nonlinear, asynchronous processes of wetland methane exchange. *Journal of Geophysical Research: Biogeosciences*, 121(1), 188–204. <https://doi.org/10.1002/2015JG003054>
- Sulova, A., & Jokar Arsanjani, J. (2020). Exploratory analysis of driving force of wildfires in Australia: An application of machine learning within Google Earth engine. *Remote Sensing*, 13(1), 10. <https://doi.org/10.3390/rs13010010>
- Sun, Y., Frankenberg, C., Wood, J. D., Schimel, D. S., Jung, M., Guanter, L., et al. (2017). OCO-2 advances photosynthesis observation from space via solar-induced chlorophyll fluorescence. *Science*, 358(6360), eaam5747. <https://doi.org/10.1126/science.aam5747>
- Sutton-Grier, A. E., & Megonigal, J. P. (2011). Plant species traits regulate methane production in freshwater wetland soils. *Soil Biology and Biochemistry*, 43(2), 413–420. <https://doi.org/10.1016/j.soilbio.2010.11.009>
- Thorne, K., MacDonald, G., Guntenspergen, G., Ambrose, R., Buffington, K., Dugger, B., et al. (2018). US Pacific coastal wetland resilience and vulnerability to sea-level rise. *Science Advances*, 4(2), eaao3270. <https://doi.org/10.1126/sciadv.aao3270>
- Thornton, P. E., Running, S. W., & White, M. A. (1997). Generating surfaces of daily meteorological variables over large regions of complex terrain. *Journal of Hydrology*, 190(3–4), 214–251. [https://doi.org/10.1016/S0022-1694\(96\)03128-9](https://doi.org/10.1016/S0022-1694(96)03128-9)
- Tiner, R. (1997). NWI maps: Basic information on the nation's wetlands. *BioScience*, 47(5), 269. <https://doi.org/10.2307/1313186>
- Tramontana, G., Ichii, K., Camps-Valls, G., Tomelleri, E., & Papale, D. (2015). Uncertainty analysis of gross primary production upscaling using Random Forests, remote sensing and eddy covariance data. *Remote Sensing of Environment*, 168, 360–373. <https://doi.org/10.1016/j.rse.2015.07.015>
- Tramontana, G., Jung, M., Schwalm, C. R., Ichii, K., Camps-Valls, G., Ráduly, B., et al. (2016). Predicting carbon dioxide and energy fluxes across global FLUXNET sites with regression algorithms. *Biogeosciences*, 13(14), 4291–4313. <https://doi.org/10.5194/bg-13-4291-2016>

- Trettin, C. C., Kolka, R. K., Marsh, A. S., Bansal, S., Lilleskov, E. A., Megonigal, P., et al. (2020). Wetland and hydric soils. In R. V. Pouyat, D. S. Page-Dumroese, T. Patel-Weyand, & L. H. Geiser (Eds.), *Forest and Rangeland Soils of the United States Under Changing Conditions* (pp. 99–126). Springer Nature.
- Turetsky, M. R., Kotowska, A., Bubier, J., Dise, N. B., Crill, P., Hornibrook, E. R., et al. (2014). A synthesis of methane emissions from 71 northern, temperate, and subtropical wetlands. *Global Change Biology*, 20(7), 2183–2197. <https://doi.org/10.1111/gcb.12580>
- Turner, A. J., Jacob, D. J., Wecht, K. J., Maasakkers, J. D., Lundgren, E., Andrews, A. E., et al. (2015). Estimating global and North American methane emissions with high spatial resolution using GOSAT satellite data. *Atmospheric Chemistry and Physics*, 15(12), 7049–7069. <https://doi.org/10.5194/acp-15-7049-2015>
- van der Valk, A. (2012). *The biology of freshwater wetlands*. Oxford University Press.
- Walter, B. P., Heimann, M., & Matthews, E. (2001). Modeling modern methane emissions from natural wetlands: 1. Model description and results. *Journal of Geophysical Research*, 106(D24), 34189–34206. <https://doi.org/10.1029/2001JD900165>
- Wang, H., Dai, Z., Krauss, K. W., Trettin, C. C., Noe, G. B., Burton, A. J., & Ward, E. J. (2023). Modeling impacts of saltwater intrusion on methane and nitrous oxide emissions in tidal forested wetlands. *Ecological Applications*, e2858. <https://doi.org/10.1002/eap.2858>
- Wang, H., Ho, M., Flanagan, N., & Richardson, C. J. (2021). The effects of hydrological management on methane emissions from southeastern shrub bogs of the USA. *Wetlands*, 41(7), 87. <https://doi.org/10.1007/s13157-021-01486-7>
- Wang, H., Richardson, C. J., & Ho, M. (2015). Dual controls on carbon loss during drought in peatlands. *Nature Climate Change*, 5(6), 584–587. <https://doi.org/10.1038/nclimate2643>
- Wang, Z., Zeng, D., & Patrick, W. H. (1996). Methane emissions from natural wetlands. *Environmental Monitoring and Assessment*, 42(1–2), 143–161. <https://doi.org/10.1007/BF00394047>
- Ward, S. E., Ostle, N. J., Oakley, S., Quirk, H., Henrys, P. A., & Bardgett, R. D. (2013). Warming effects on greenhouse gas fluxes in peatlands are modulated by vegetation composition. *Ecology Letters*, 16(10), 1285–1293. <https://doi.org/10.1111/ele.12167>
- Watts, W. R. (1975). Air and soil temperature differences in controlled environments, as a consequence of high radiant flux densities and of day/night temperature changes. *Plant and Soil*, 42(1), 299–303. <https://doi.org/10.1007/BF02186991>
- Whalen, S. C., & Reeburgh, W. S. (1992). Interannual variations in tundra methane emission: A 4-year time series at fixed sites. *Global Biogeochemical Cycles*, 6(2), 139–159. <https://doi.org/10.1029/92GB00430>
- Whalen, S. C., & Reeburgh, W. S. (1996). Moisture and temperature sensitivity of CH<sub>4</sub> oxidation in boreal soils. *Soil Biology and Biochemistry*, 28(10–11), 1271–1281. [https://doi.org/10.1016/S0038-0717\(96\)00139-3](https://doi.org/10.1016/S0038-0717(96)00139-3)
- White, E. E., Ury, E. A., Bernhardt, E. S., & Yang, X. (2021). Climate change driving widespread loss of coastal forested wetlands throughout the North American coastal plain. *Ecosystems*, 25(4), 1–16. <https://doi.org/10.1007/s10021-021-00686-w>
- Wilén, B. O., & Bates, M. K. (1995). The US Fish and Wildlife Service's national wetlands inventory project. In C. M. Finlayson & A. G. van der Valk (Eds.), *Classification and inventory of the world's wetlands* (pp. 153–169). Springer. [https://doi.org/10.1007/978-94-011-0427-2\\_13](https://doi.org/10.1007/978-94-011-0427-2_13)
- Wu, Z., Ahlström, A., Smith, B., Ardö, J., Eklundh, L., Fensholt, R., & Lehsten, V. (2017). Climate data induced uncertainty in model-based estimations of terrestrial primary productivity. *Environmental Research Letters*, 12(6), 064013. <https://doi.org/10.1088/1748-9326/aa6fd8>
- Wuebbles, D. J., & Hayhoe, K. (2002). Atmospheric methane and global change. *Earth-Science Reviews*, 57(3–4), 177–210. [https://doi.org/10.1016/S0012-8252\(01\)00062-9](https://doi.org/10.1016/S0012-8252(01)00062-9)
- Xu, T., Guo, Z., Liu, S., He, X., Meng, Y., Xu, Z., et al. (2018). Evaluating different machine learning methods for upscaling evapotranspiration from flux towers to the regional scale. *Journal of Geophysical Research: Atmospheres*, 123(16), 8674–8690. <https://doi.org/10.1029/2018JD028447>
- Yang, J., Liu, J., Hu, X., Li, X., Wang, Y., & Li, H. (2013). Effect of water table level on CO<sub>2</sub>, CH<sub>4</sub> and N<sub>2</sub>O emissions in a freshwater marsh of Northeast China. *Soil Biology and Biochemistry*, 61, 52–60. <https://doi.org/10.1016/j.soilbio.2013.02.009>
- Ye, R., Jin, Q., Bohannon, B., Keller, J. K., McAllister, S. A., & Bridgman, S. D. (2012). pH controls over anaerobic carbon mineralization, the efficiency of methane production, and methanogenic pathways in peatlands across an ombrotrophic–minerotrophic gradient. *Soil Biology and Biochemistry*, 54, 36–47. <https://doi.org/10.1016/j.soilbio.2012.05.015>
- Yuan, K., Li, F., McNicol, G., Chen, M., Hoyt, A., Knox, S., et al. (2024). Boreal–Arctic wetland methane emissions modulated by warming and vegetation activity. *Nature Climate Change*, 14(3), 282–288. <https://doi.org/10.1038/s41558-024-01933-3>
- Yuan, K., Zhu, Q., Li, F., Riley, W. J., Torn, M., Chu, H., et al. (2022). Causality guided machine learning model on wetland CH<sub>4</sub> emissions across global wetlands. *Agricultural and Forest Meteorology*, 324, 109115. <https://doi.org/10.1016/j.agrformet.2022.109115>
- Yvon-Durocher, G., Allen, A. P., Bastviken, D., Conrad, R., Gudas, C., St-Pierre, A., et al. (2014). Methane fluxes show consistent temperature dependence across microbial to ecosystem scales. *Nature*, 507(7493), 488–491. <https://doi.org/10.1038/nature13164>
- Zeng, C., Yang, L., & Zhu, A. X. (2017). Construction of membership functions for soil mapping using the partial dependence of soil on environmental covariates calculated by random forest. *Soil Science Society of America Journal*, 81(2), 341–353. <https://doi.org/10.2136/sssaj2016.06.0195>
- Zhang, L., Dumont, M. G., Bodelier, P. L., Adams, J. M., He, D., & Chu, H. (2020). DNA stable-isotope probing highlights the effects of temperature on functionally active methanotrophs in natural wetlands. *Soil Biology and Biochemistry*, 149, 107954. <https://doi.org/10.1016/j.soilbio.2020.107954>
- Zhang, Y., Jacob, D. J., Lu, X., Maasakkers, J. D., Scarpelli, T. R., Sheng, J. X., et al. (2021). Attribution of the accelerating increase in atmospheric methane during 2010–2018 by inverse analysis of GOSAT observations. *Atmospheric Chemistry and Physics*, 21(5), 3643–3666. <https://doi.org/10.5194/acp-21-3643-2021>
- Zhang, Y., Qian, B., & Hong, G. (2020). A long-term, 1-km resolution daily meteorological dataset for modeling and mapping permafrost in Canada. *Atmosphere*, 11(12), 1363. <https://doi.org/10.3390/atmos11121363>
- Zhang, Y., Xiao, X., Wu, X., Zhou, S., Zhang, G., Qin, Y., & Dong, J. (2017). A global moderate resolution dataset of gross primary production of vegetation for 2000–2016. *Scientific Data*, 4(1), 1–13. <https://doi.org/10.1038/sdata.2017.165>
- Zhang, Z., Fluet-Chouinard, E., Jensen, K., McDonald, K., Hugelius, G., Gumbrecht, T., et al. (2021). Development of a global dataset of wetland area and dynamics for methane modeling (WAD2M). *Earth System Science Data*, 13(5), 2001–2023. <https://doi.org/10.5194/essd-13-2001-2021>
- Zhang, Z., Zimmermann, N. E., Stenke, A., Li, X., Hodson, E. L., Zhu, G., et al. (2017). Emerging role of wetland methane emissions in driving 21st century climate change. *Proceedings of the National Academy of Sciences of the United States of America*, 114(36), 9647–9652. <https://doi.org/10.1073/pnas.1618765114>
- Zhu, X., Zhuang, Q., Chen, M., Sirin, A., Melillo, J., Kicklighter, D., et al. (2011). Rising methane emissions in response to climate change in Northern Eurasia during the 21st century. *Environmental Research Letters*, 6(4), 045211. <https://doi.org/10.1088/1748-9326/6/4/045211>
- Zhu, X., Zhuang, Q., Qin, Z., Glagolev, M., & Song, L. (2013). Estimating wetland methane emissions from the northern high latitudes from 1990 to 2009 using artificial neural networks. *Global Biogeochemical Cycles*, 27(2), 592–604. <https://doi.org/10.1002/gbc.20052>

- Zhuang, Q., Melillo, J. M., Kicklighter, D. W., Prinn, R. G., McGuire, A. D., Steudler, P. A., et al. (2004). Methane fluxes between terrestrial ecosystems and the atmosphere at northern high latitudes during the past century: A retrospective analysis with a process-based biogeochemistry model. *Global Biogeochemical Cycles*, *18*(3). <https://doi.org/10.1029/2004GB002239>
- Zimov, S. A., Schuur, E. A., & Chapin, F. S., III. (2006). Permafrost and the global carbon budget. *Science*, *312*(5780), 1612–1613. <https://doi.org/10.1126/science.1128908>
- Zinder, S. H., Anguish, T., & Cardwell, S. C. (1984). Effects of temperature on methanogenesis in a thermophilic (58°C) anaerobic digester. *Applied and Environmental Microbiology*, *47*(4), 808–813. <https://doi.org/10.1128/aem.47.4.808-813.1984>
- Zou, J., Ziegler, A. D., Chen, D., McNicol, G., Ciais, P., Jiang, X., et al. (2022). Rewetting global wetlands effectively reduces major greenhouse gas emissions. *Nature Geoscience*, *15*(8), 627–632. <https://doi.org/10.1038/s41561-022-00989-0>